Lesson 10:
Nanostructures on substrates and in matrices
(Control of size and number of nanoparticles on substrates and in matrices: nucleation and growth thermodynamics and kinetics (basic concepts and experimental data); Ripening and Coalescence: basic rate equations and experimental data; Typical activation energies and diffusion coefficients)

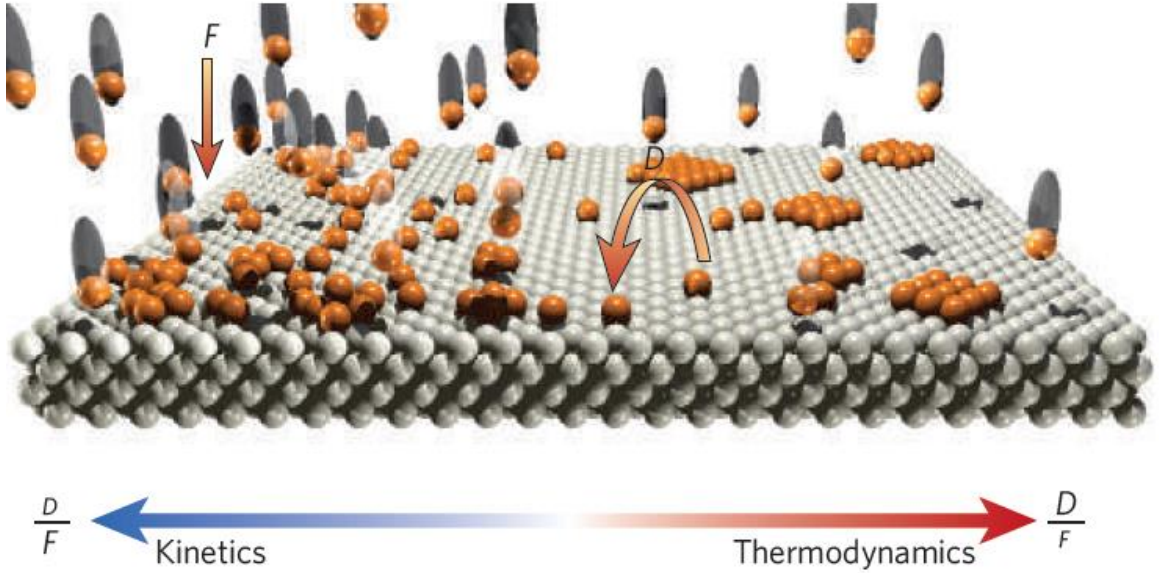

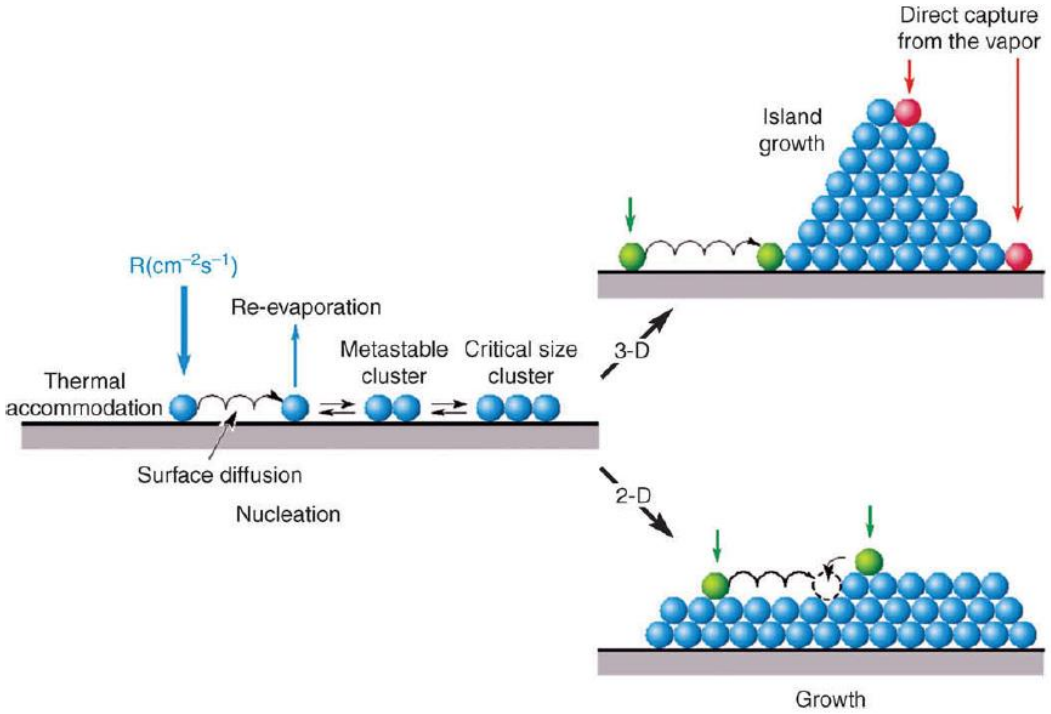

Coverage / Mechanism	θ < 1 ML	1 < θ < 2 ML	θ > 2 ML	Examples
3D island growth				Metals on SiO_2
2D layer growth				Cu/Cu, Si/Si, GaAs/GaAs
S-K growth				In/Si, Ge/Si InGaAs/GaAs

D=Surface Diffusion Coefficient (cm^2/s)
F=Flux of impinging atoms ($atoms/cm^2s$)

Controlling the self-organization mechanisms

- **The Ripening and Coalescence processes are the main growth mechanisms for metal NPs leading to morphological and structural evolution of the NPs.**
- **The control of the NPs Ripening and Coalescence processes can lead to NPs with desired size, morphology and structure**

Ripening

Coalescence

Driving Force: Minimization of the Total Surface Energy of the System

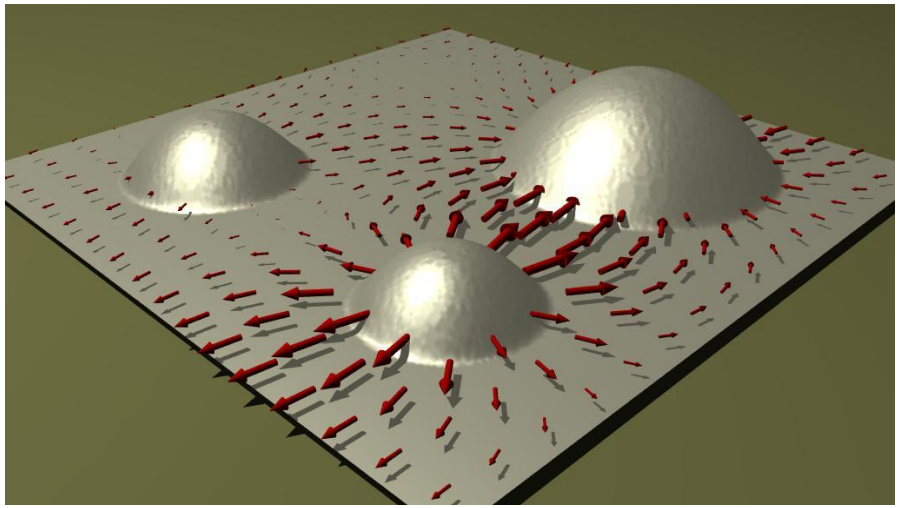

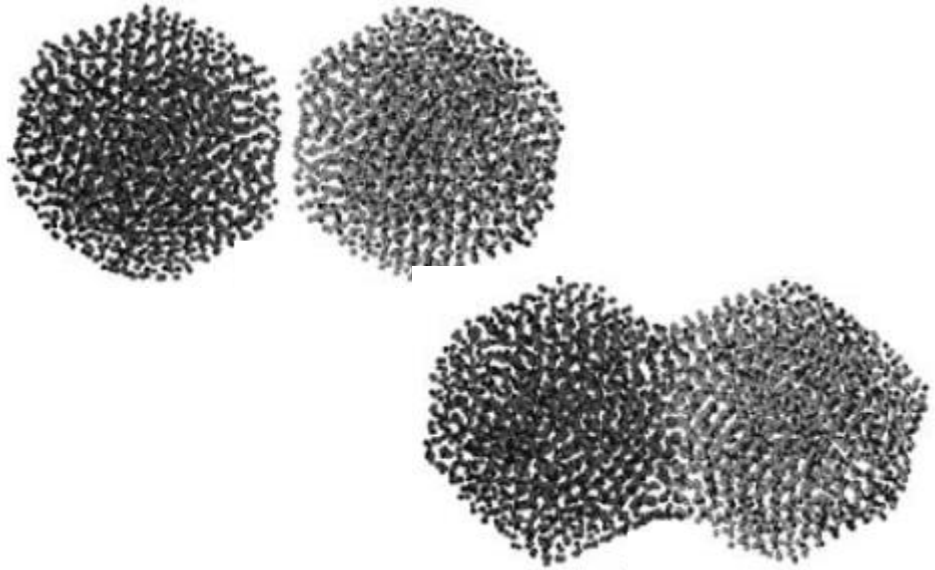

K. -N. Tu, J. W. Mayer, L. C. Feldman, «Electronic Thin Fils Science» , MacMilian 1992

The Ripening process: basics

The ripening process involves an atomic diffusion from smaller particles to larger particles. This is due to the Gibbs-Thompson effect, i. e. the atomic pressure vapor is higher around smaller particles. So, the smaller particles shrink and dissolve (in atomic form) and these atoms are captured by larger particles placed within the atomic diffusion length

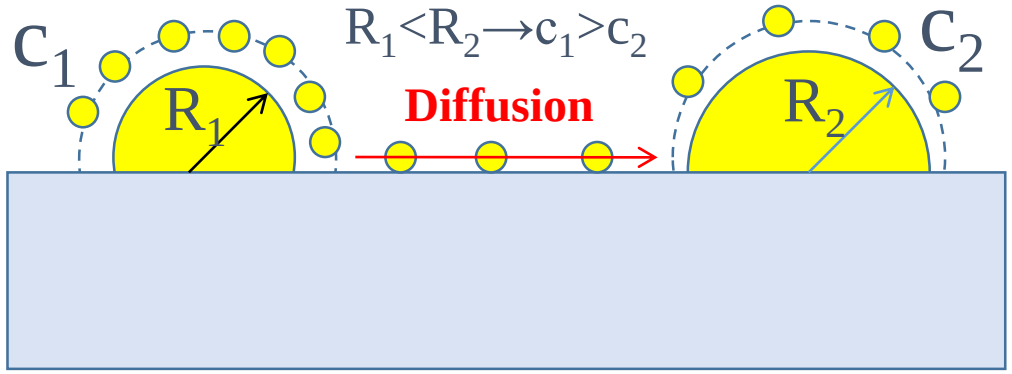

Gibbs-Thompson effect

$$p \propto exp[2\gamma_S \Omega / kTR]$$

Diffusion Length

$$L_D \sim \sqrt{D_S t}$$

Diffusion Coefficient

$$D_S \sim exp[-E_A / kT]$$

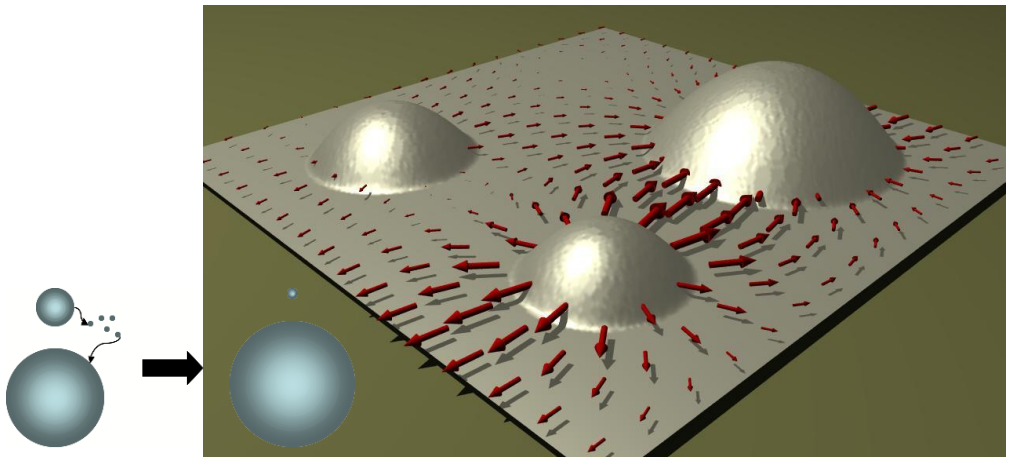

The Coalescence process: basics

The coalescence process involves the touching (contact) of two or more particles, deforming their surfaces, to form a particle having volume the sum of the volumes of the touching particles but surface area lower than the sum of the surface areas of the touching particles.

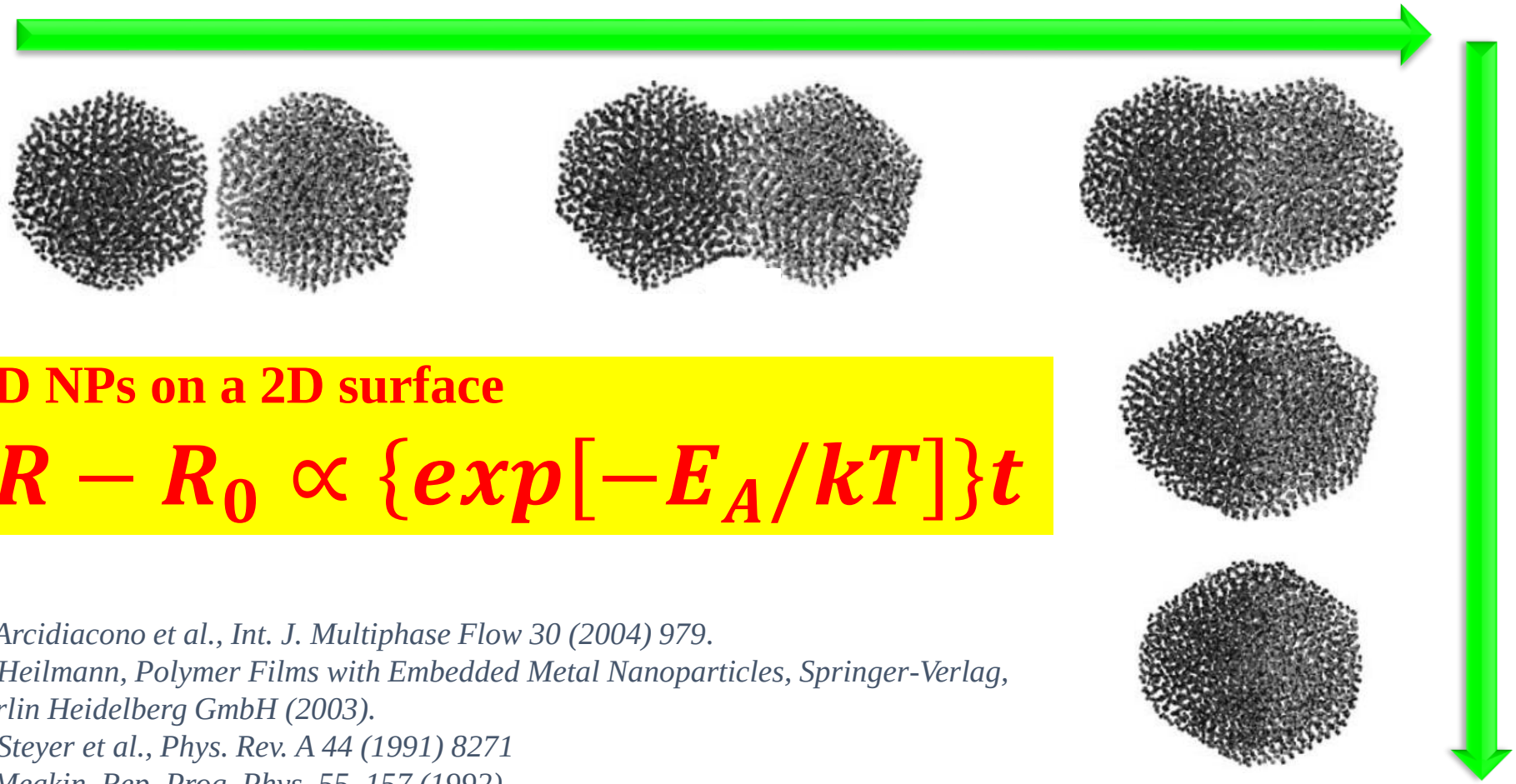

3D NPs on a 2D surface

$$R - R_0 \propto \{exp[-E_A/kT]\}t$$

S. Arcidiacono et al., Int. J. Multiphase Flow 30 (2004) 979.
A. Heilmann, Polymer Films with Embedded Metal Nanoparticles, Springer-Verlag, Berlin Heidelberg GmbH (2003).
A. Steyer et al., Phys. Rev. A 44 (1991) 8271
P. Meakin, Rep. Prog. Phys. 55, 157 (1992)

Analysys of the Ripening process of Au nanoparticles on surface

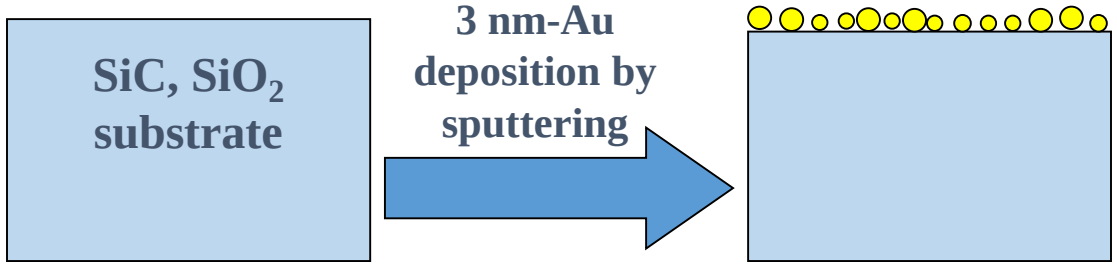

Samples preparation and microscopic structural analyses

600 °C÷800 °C annealing temperature, 300s÷3600s annealing time, Ar ambient

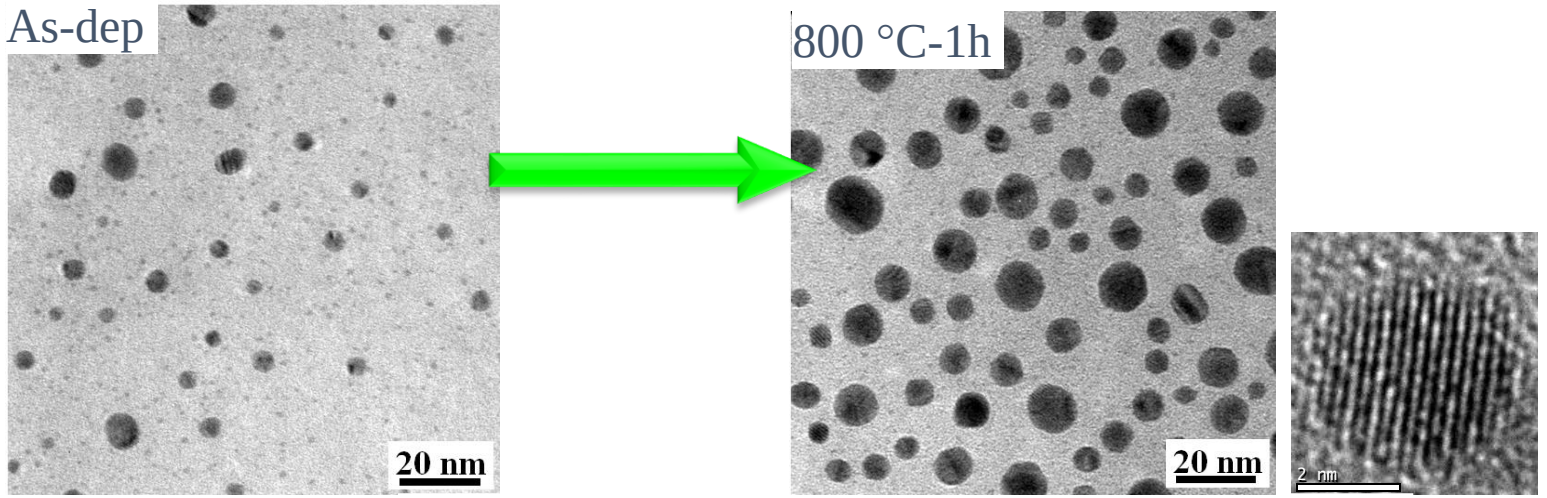

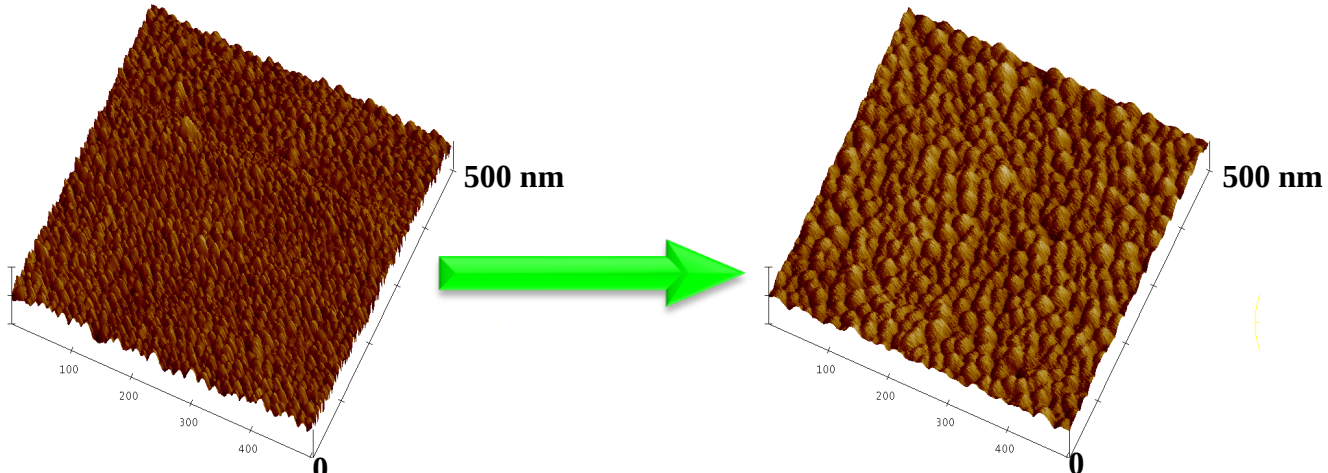

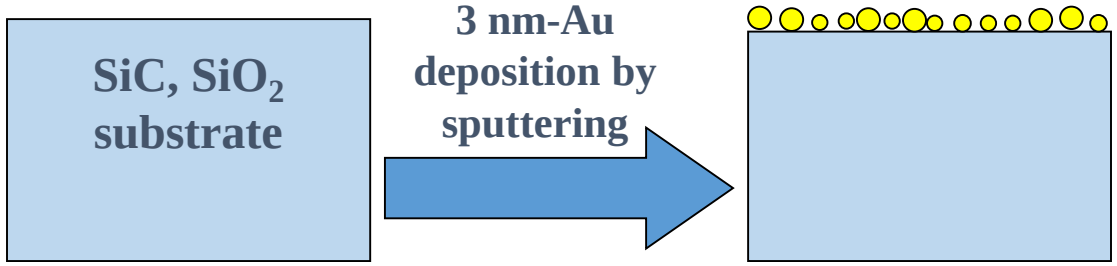

Samples preparation and microscopic structural analyses

600 °C÷800 °C annealing temperature, 300s÷3600s annealing time, Ar ambient

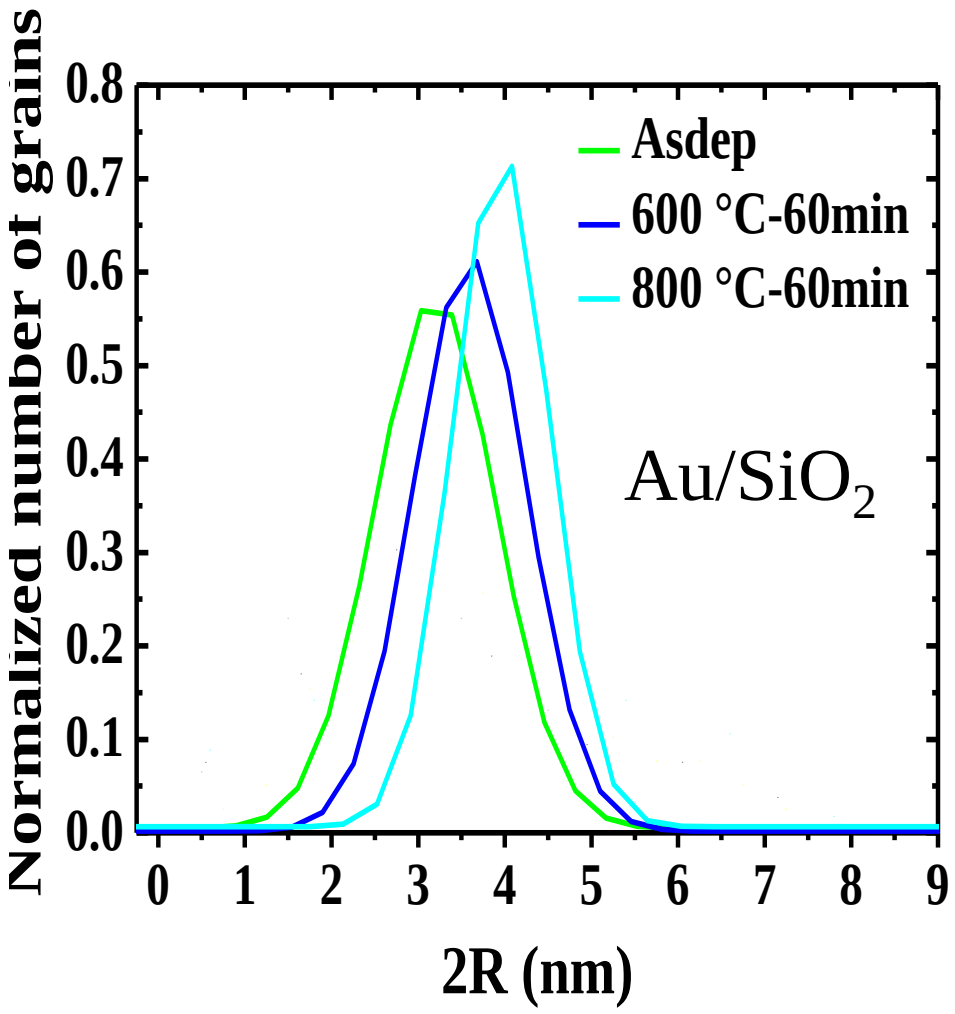

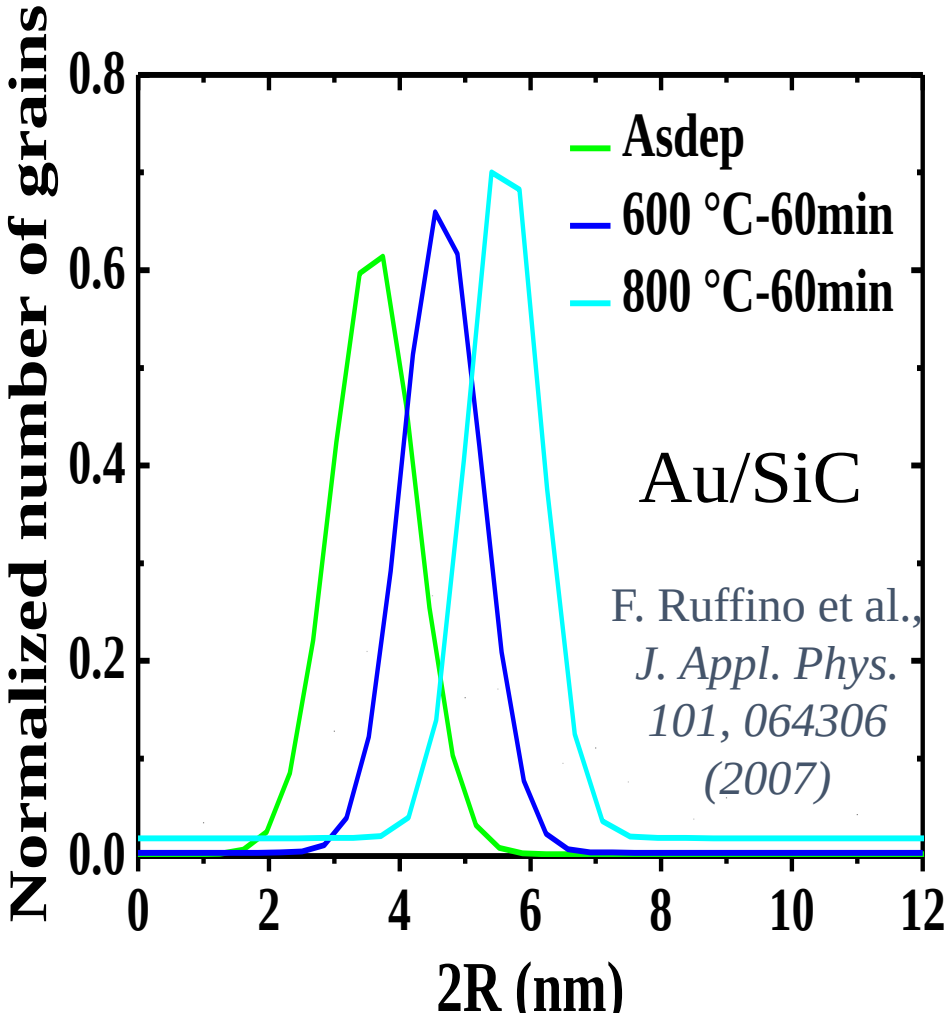

Diffusion limited ripening: solution of the rate equation (kinetic equation)

$$R^n(t) - R_0^n = Kt$$

$n = 2$ (2D/2D case) for the growth of two-dimensional (2D) particles on a surface (2D);

$n = 3$ (3D/3D case) for the growth of the three-dimensional (3D) particles embedded in a bulk matrix (3D);

$n = 4$ (3D/2D case) for the growth of three-dimensional (3D) particles on a surface (2D).

$$R^4(t) - R_0^4 = Kt \qquad K = \frac{8N_0 D_S \gamma \Omega^2}{45 k_B T \ln(L)} \qquad D_S = D_0 \exp\left[-\frac{E_A}{kT}\right]$$

I. M. Lifshitz et al. J. Phys. Chem. Solids 19, 35 (1961).
K. -N. Tu, J. W. Mayer, L. C. Feldman, «Electronic Thin Fils Science» , MacMilian 1992
M. Zinke-Allmang et al., Surf. Sci. Rep. 16, 377 (1992).

F. Ruffino et al. J. Appl. Phys. 101, 064306 (2007); Superlattices and Microstructures 44, 588 (2008)

Growth exponent

$$R^4(t) - R_0^4 = Kt$$

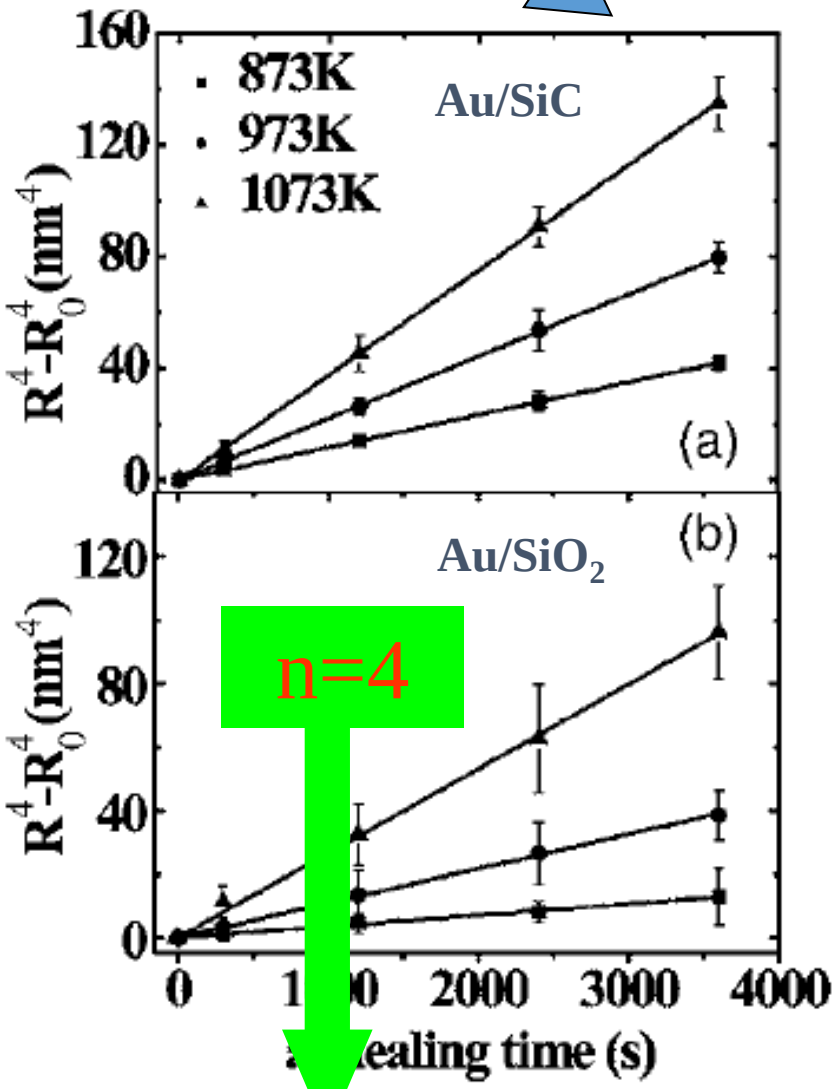

n=4

3D growth by surface diffusion

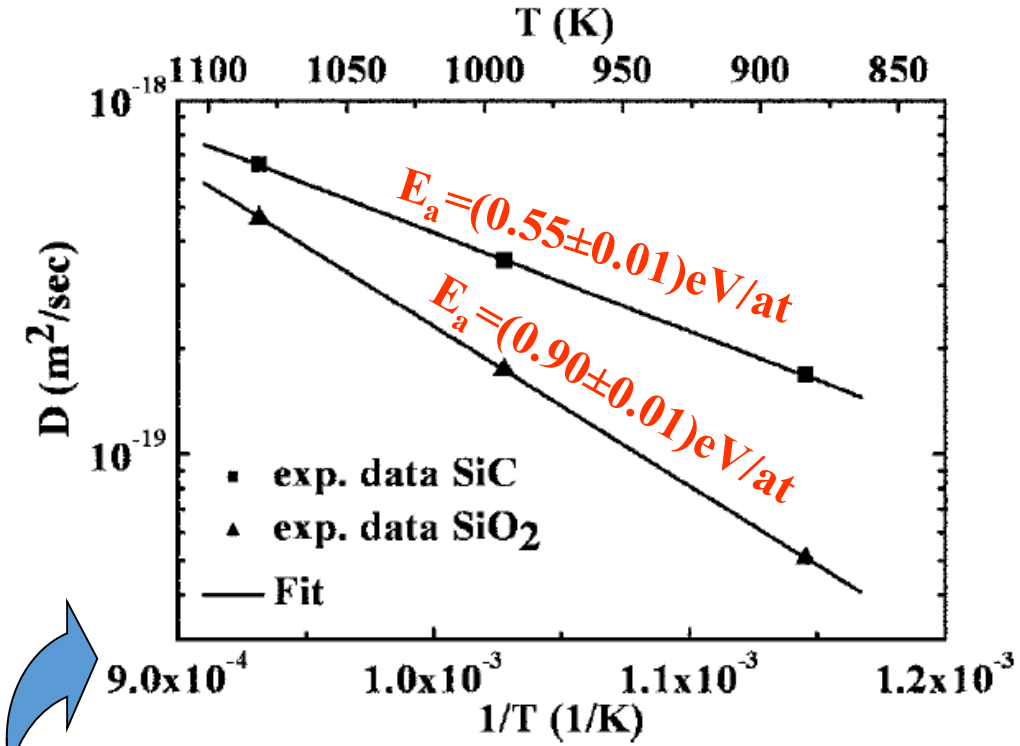

D diffusion coefficient of Au atoms on surfaces

$$D(T) = D_0 e^{-\frac{E_a}{k_B T}}$$

$$K = \frac{a_{Au}^2 D\gamma}{45\ln(3)k_B T}$$

a_{Au}=0.409 nm Au atom covalent radius

γ=1.5 J/m^2 specific interfacial energy of the Au nanocluster - air boundary

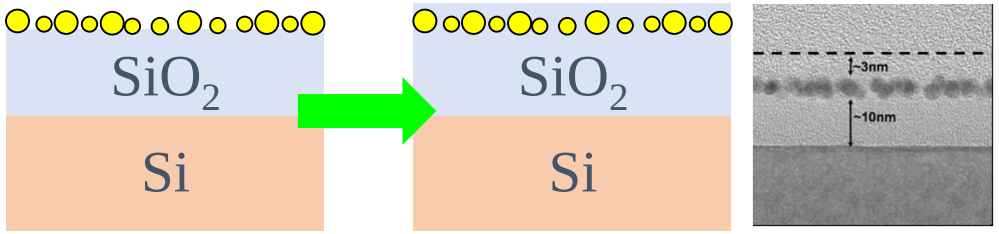

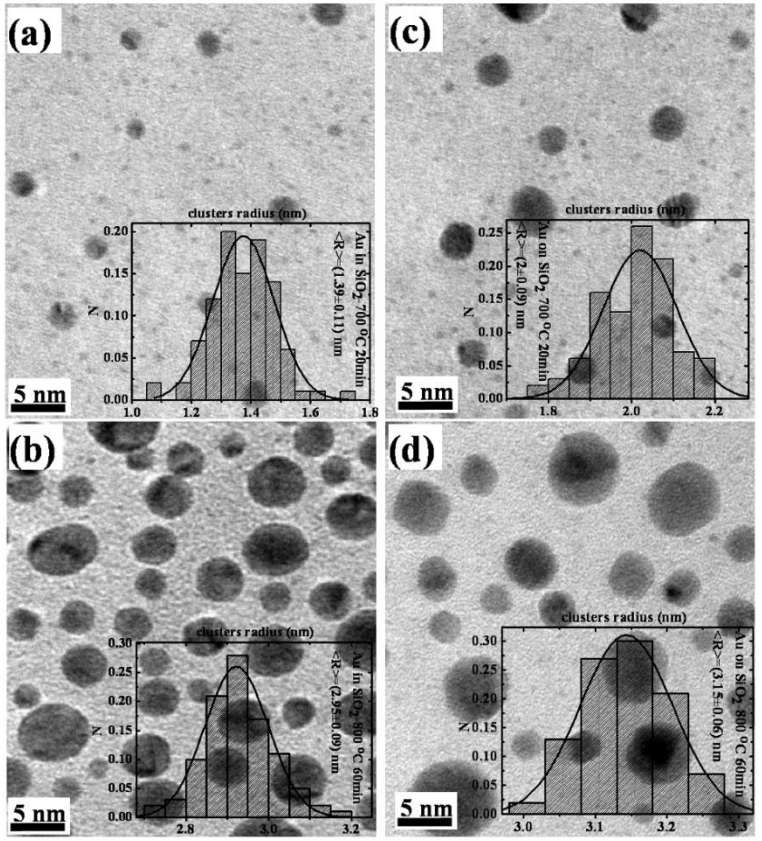

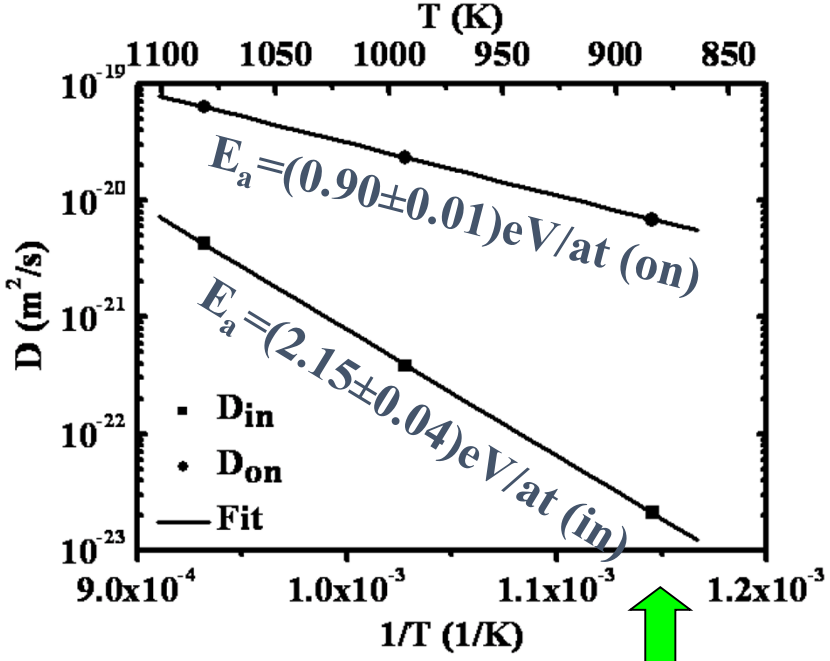

$$R^3(t) - R_0^3 = Kt$$

$$K = \frac{8C_\infty D_{IN}\gamma_S\Omega^2}{9k_BT}$$

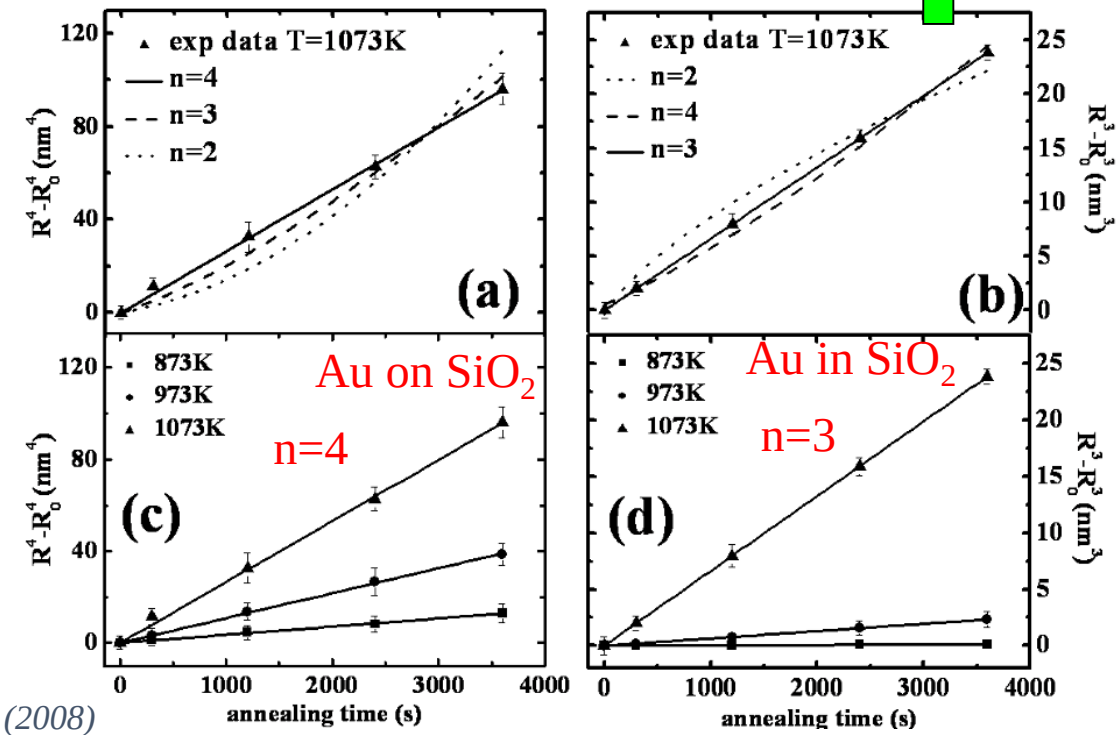

F. Ruffino et al. Superlattices and Microstructures 44, 588 (2008)

Appl. Phys. A 81, 673–677 (2005)
DOI: 10.1007/s00339-005-3254-9

Applied Physics A
Materials Science & Processing

I. BESZEDA[1,✉]
E.G. GONTIER-MOYA[2]
Á.W. IMRE[3]

Surface Ostwald-ripening and evaporation of gold beaded films on sapphire

[1] Department of Solid State Physics, University of Debrecen, 4010 Debrecen, Hungary
[2] L2MP, UMR CNRS 6137, Université Paul Cézanne Aix-Marseille III, Marseille, France
[3] Institut für Materialphysik, Westfälische Wilhelms-Universität, 48149 Münster, Germany

Received: 3 November 2004/Accepted: 2 March 2005
Published online: 10 May 2005 •

ABSTRACT The kinetics of morphological evolutions of gold nanoparticles on alumina, resulting from evaporation and surface Ostwald-ripening coarsening, have been investigated by means of Auger electron spectroscopy. When the fraction of the covered area is small, the kinetics of evaporation can be related to the desorption of adatoms. In the temperature range 943–1043 K we obtained the evaporation flux $J(\mathrm{m}^{-2}\mathrm{s}^{-1}) = 4.8 \times 10^{27}\exp[-196 \pm 9\ (\mathrm{kJ/mol})/RT]$. The experimental activation energy of evaporation of gold from a sapphire surface, $Q_{\mathrm{evap}} = 196 \pm 9$ kJ/mol, is lower than the tabulated value of enthalpy of sublimation of gold, $\Delta H_{\mathrm{subl}} = 368$ kJ/mol. At lower temperatures, in the range 623–778 K, Ostwald-ripening experiments, carried out on nanosized clusters, yield the mass transfer surface diffusion coefficients of gold on alumina, $D_{\mathrm{s}}(\mathrm{m}^2/\mathrm{s}) = 2.6 \times 10^{-14}\exp[-58 \pm 9\ (\mathrm{kJ/mol})/RT]$. These results, providing information on the evolution of granular gold films such as those used in catalysts or sensors, are compared to previous data on similar systems.

E_A (Au on Al_2O_3)=0.6 eV

THE JOURNAL OF CHEMICAL PHYSICS **138**, 184710 (2013)

Adsorption and diffusion of the Rh and Au adatom on graphene moiré/Ru(0001)

Lymarie Semidey-Flecha,[1] Dieh Teng,[2] Bradley F. Habenicht,[1] David S. Sholl,[2] and Ye Xu[1,a)]

[1]*Center for Nanophase Materials Sciences, Oak Ridge National Laboratory, Oak Ridge, Tennessee 37831, USA*

[2]*School of Chemical & Biomolecular Engineering, Georgia Institute of Technology, Atlanta, Georgia 30332, USA*

(Received 29 January 2013; accepted 19 April 2013; published online 14 May 2013)

Detailed density functional theory calculations have been performed to investigate the adsorption and diffusion of the Rh and Au adatom on the graphene moiré superstructure on Ru(0001). The adsorption energies of each adatom in all of the non-equivalent C-top and C_6 ring center sites on the graphene moiré have been calculated. The resulting potential energy surfaces encompass the entire graphene moiré unit cell and shows that the adsorption of both Rh_1 and Au_1 is most stable in the fcc region on the graphene moiré. The minimum-energy diffusion path between adjacent moiré cells is identified to run mostly directly between the fcc and hcp regions for Au_1, but deviates toward the mound region for Rh_1. The global diffusion barrier is estimated to be 0.53 eV for Rh_1 and 0.71 eV for Au_1, corresponding to a hopping rate between adjacent moiré cells of $\sim 10^3$ s^{-1} and ~ 1 s^{-1} at 298 K, respectively. The consequences of different hopping rates to cluster nucleation have been explored by performing Monte Carlo-based statistical analysis, which suggests that diffusing species other than adatoms need to be taken into account to develop an accurate description of cluster nucleation and growth on this surface.
 [http://dx.doi.org/10.1063/1.4803893]

E_A (Au on graphene/Ru(0001))=0.71 eV

Analysys of the Coalescence process of Au nanoparticles on surface

Samples preparation and microscopic analyses

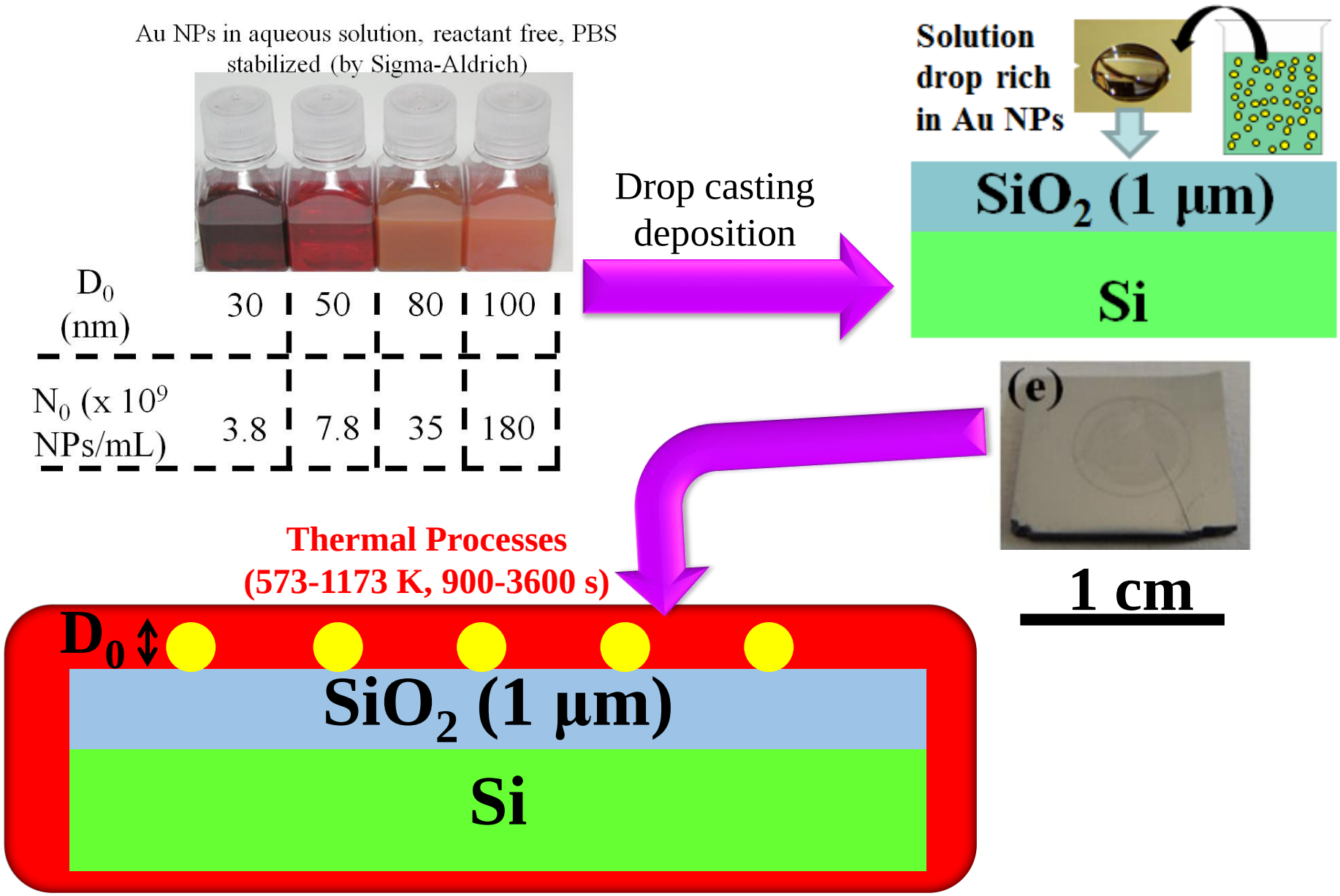

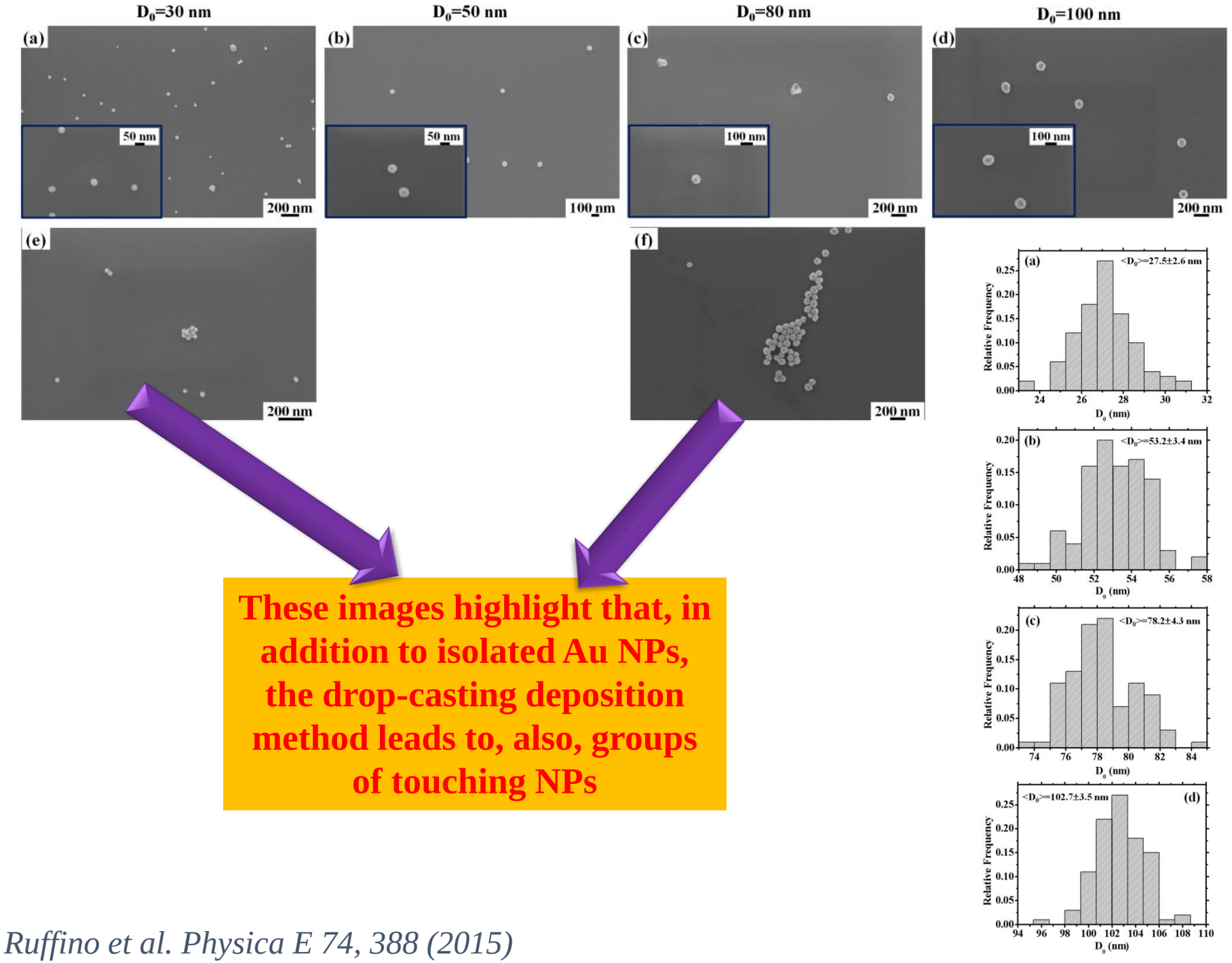

These images highlight that, in addition to isolated Au NPs, the drop-casting deposition method leads to, also, groups of touching NPs

F. Ruffino et al. Physica E 74, 388 (2015)

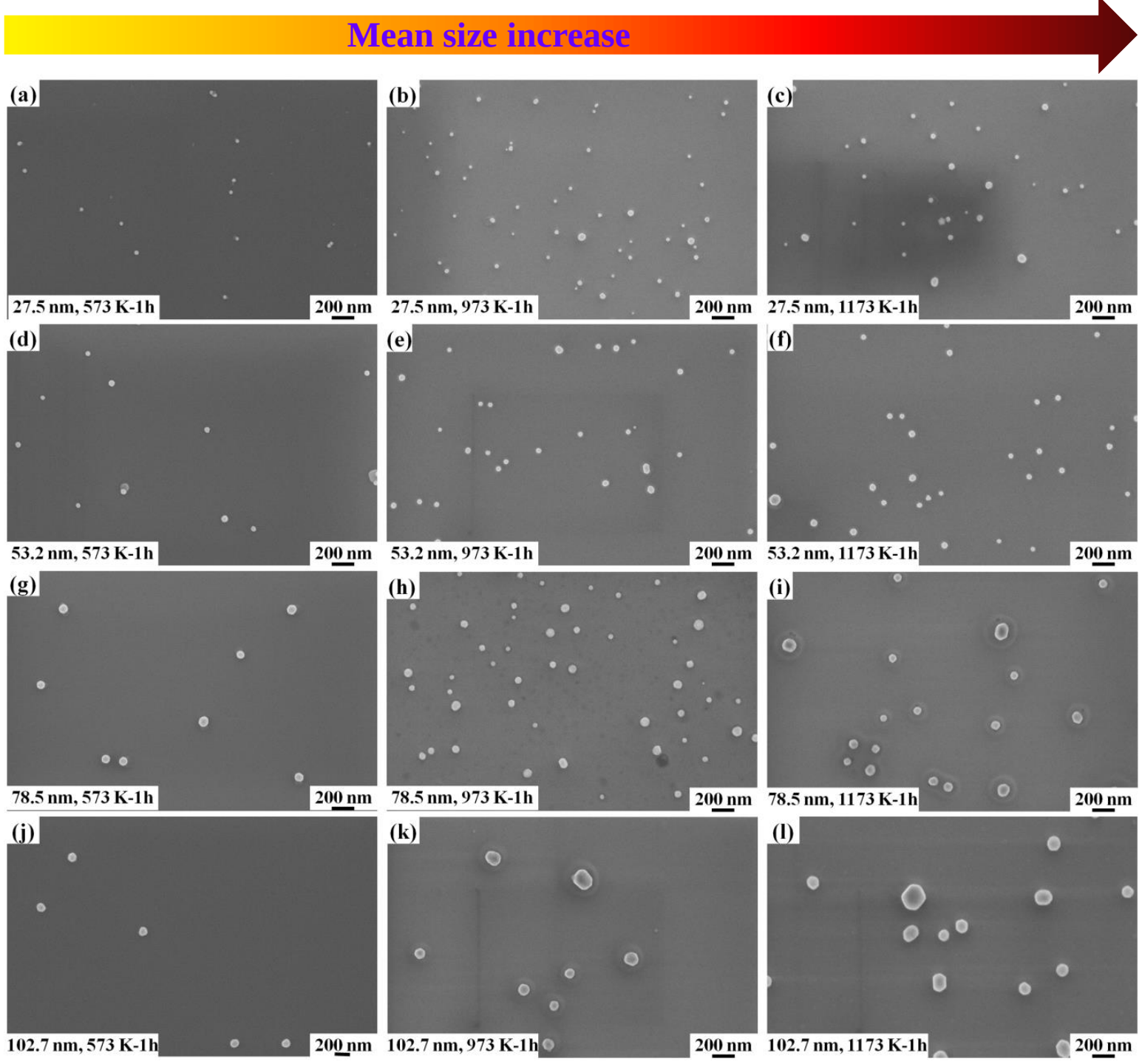
Mean size increase
(a)
27.5 nm, 573 K-1h
200 nm
(b)
27.5 nm, 973 K-1h
200 nm
(c)
27.5 nm, 1173 K-1h
200 nm
(d)
53.2 nm, 573 K-1h
200 nm
(e)
53.2 nm, 973 K-1h
200 nm
(f)
53.2 nm, 1173 K-1h
200 nm
(g)
78.5 nm, 573 K-1h
200 nm
(h)
78.5 nm, 973 K-1h
200 nm
(i)
78.5 nm, 1173 K-1h
200 nm
(j)
102.7 nm, 573 K-1h
200 nm
(k)
102.7 nm, 973 K-1h
200 nm
(l)
102.7 nm, 1173 K-1h
200 nm

F. Ruffino et al. Physica E 74, 388 (2015)

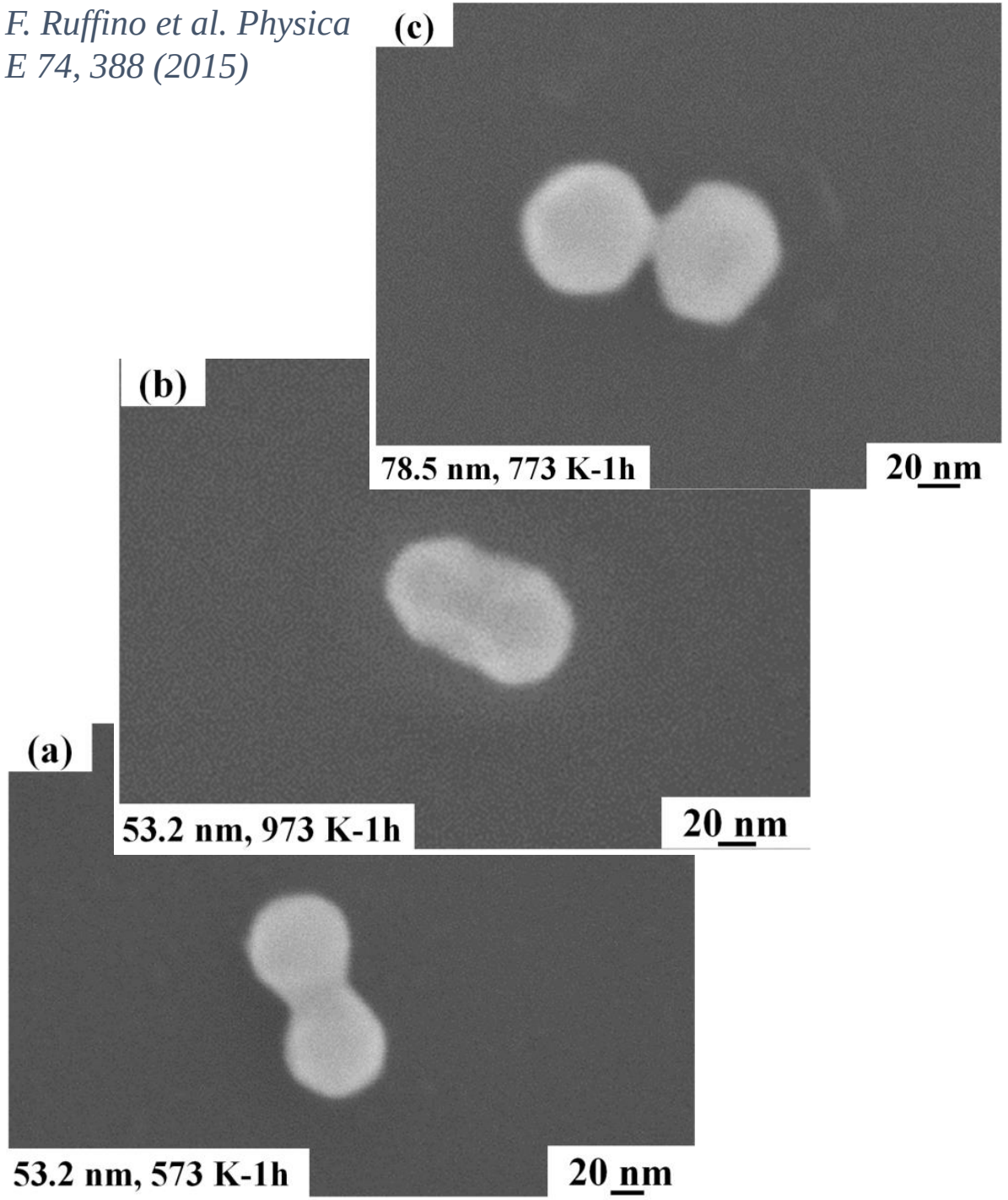

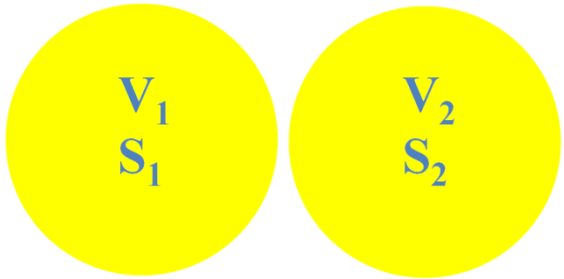

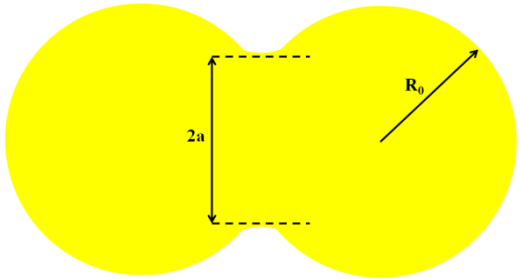

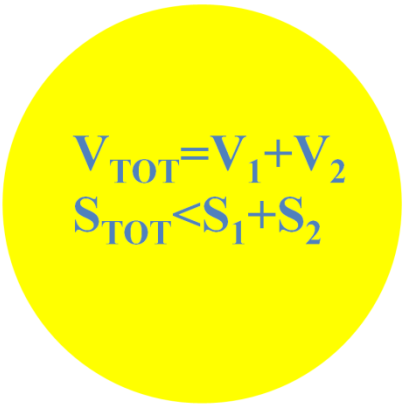

The coalescence process involves the touching (contact) of single particles, deforming their surfaces (neck formation), to form a particle having volume the sum of the volumes but surface area lower than the sum of the surface areas.

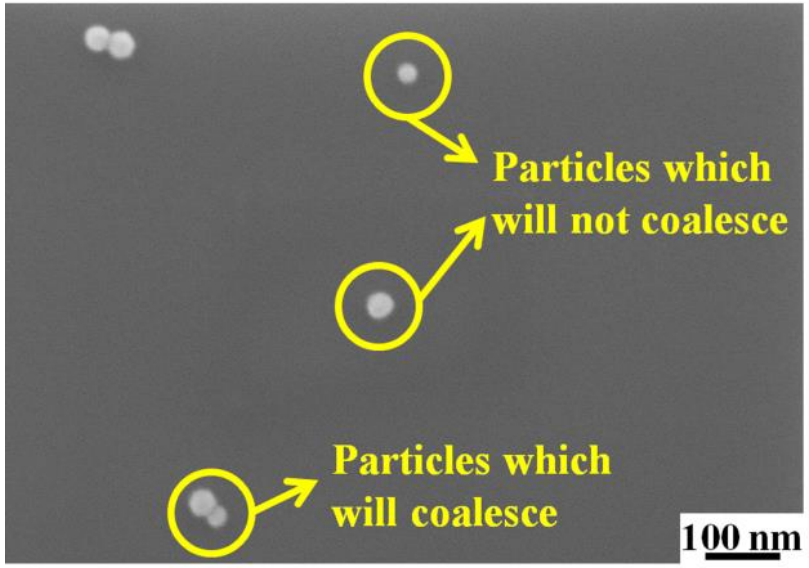

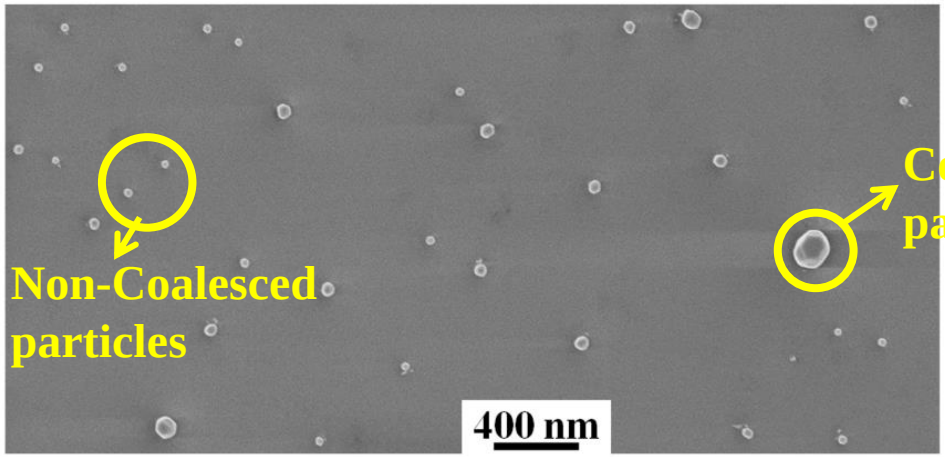

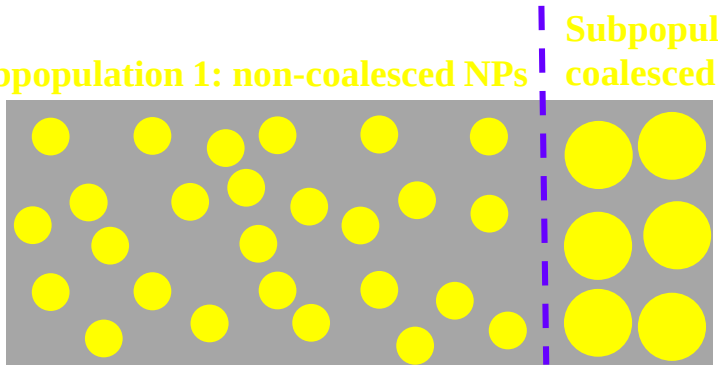

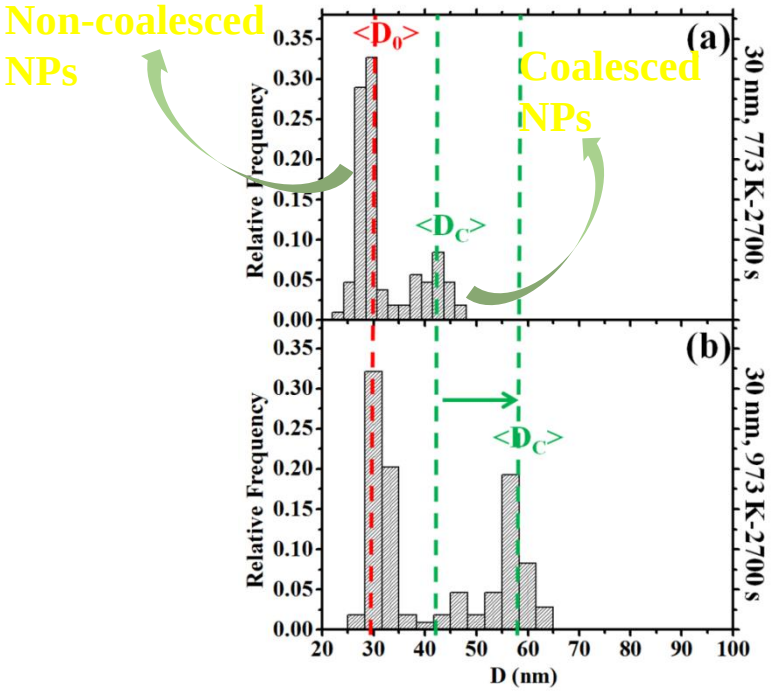

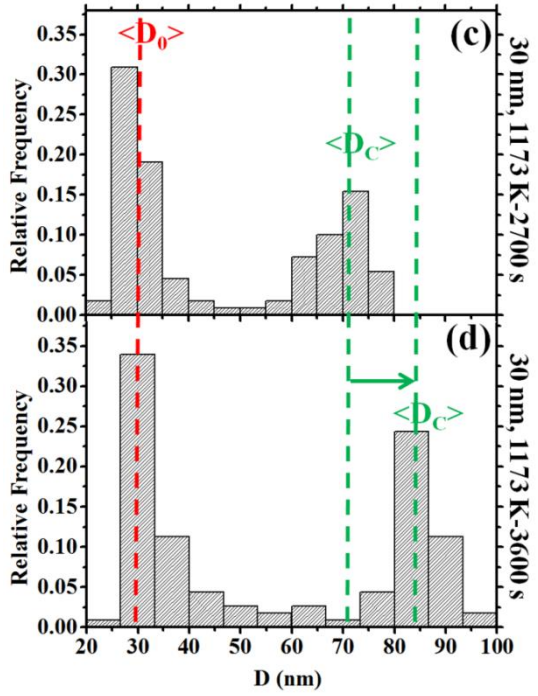

Bimodal size distributions

Coalescence: solution of the rate equation (kinetic equation)

SD: Surface Diffusion;
GBD: Grain Boundary Diffusion;
EC: Evaporation and Condenation;
VDS: Volume Diffusion from the Surface;
VDV: Volume Diffusion from the Interior.
$<D_0>$: mean diameter of the as-deposited NPs;
$<D_C>$: mean diameter of the coalesced NPs;
t: annealing time;
T: absolute annealing temperature;
E_A: activation energy for the NPs coalescence process.

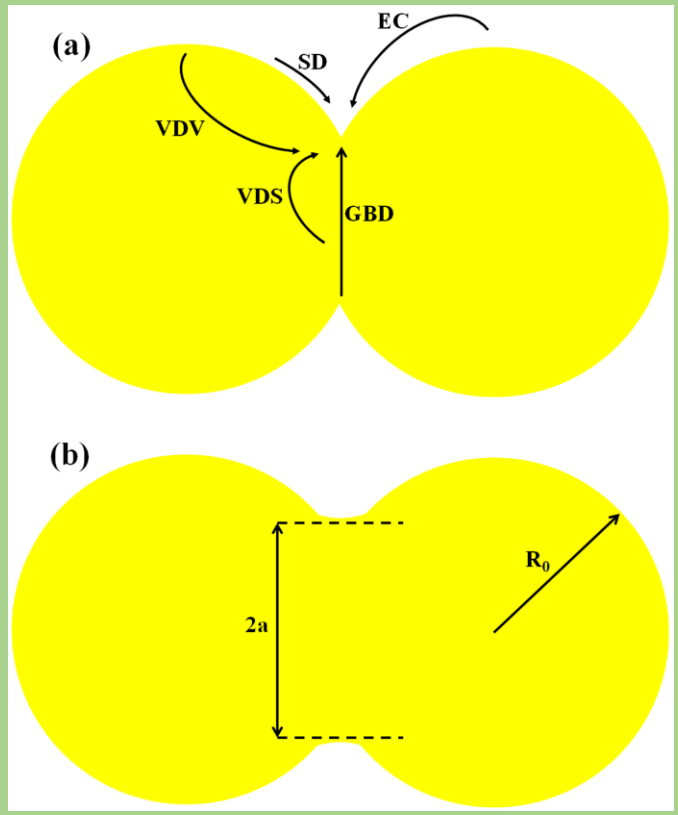

$$< D_C >=< D_0 > +\gamma t$$

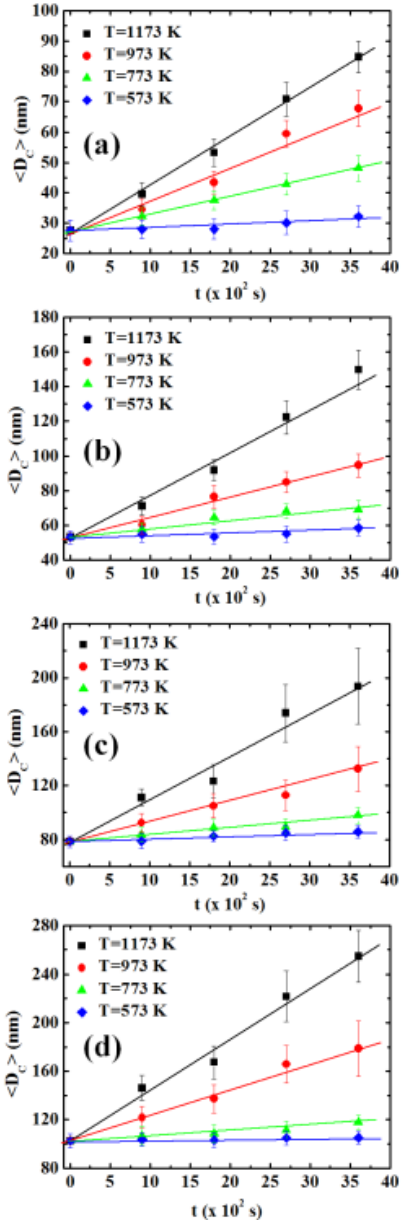

A. Steyer et al., Phys. Rev. A 44 (1991) 8271; P. Meakin, Rep. Prog. Phys. 35 (1992) 157; A. Heilmann, Polymer Films with Embedded Metal Nanoparticles, Springer-Verlag, Berlin Heidelberg GmbH (2003);
S. Arcidiacono et al., Int. J. Multiphase Flow 30 (2004) 979.

Available online at www.sciencedirect.com
SCIENCE DIRECT®
International Journal of Multiphase Flow 30 (2004) 979–994
International Journal of Multiphase Flow
www.elsevier.com/locate/ijmulflow

On the coalescence of gold nanoparticles ☆

S. Arcidiacono [a], N.R. Bieri [a], D. Poulikakos [a,*], C.P. Grigoropoulos [b]

The energy change of the system can be written as

$$\frac{dE}{dt} = \frac{d(E_{bulk} + E_{surface})}{dt} = 2NC_v \frac{dT}{dt} + \sigma_{sv} \frac{da}{dt} = 0 \quad (2)$$

where C_v is the constant-volume heat capacity, σ_{sv} is the solid–vapor surface tension, T and a are the temperature and the surface of the two coalescing particles at time t.

The surface area reduction by sintering can be described by the linear law of Koch and Friedlander (1990):

$$\frac{da}{dt} = -\frac{1}{\tau}(a - a_s) \quad (3)$$

where a_s is the surface area of the final sphere (assumed in the analytical solution) and τ the characteristic sintering time that will be defined later in this section. The relation above was

Finally, the derivative of the particle temperature can be expressed as

$$\frac{dT}{dt} = -\frac{\sigma_{sv}}{2NC_v} \frac{da}{dt}$$

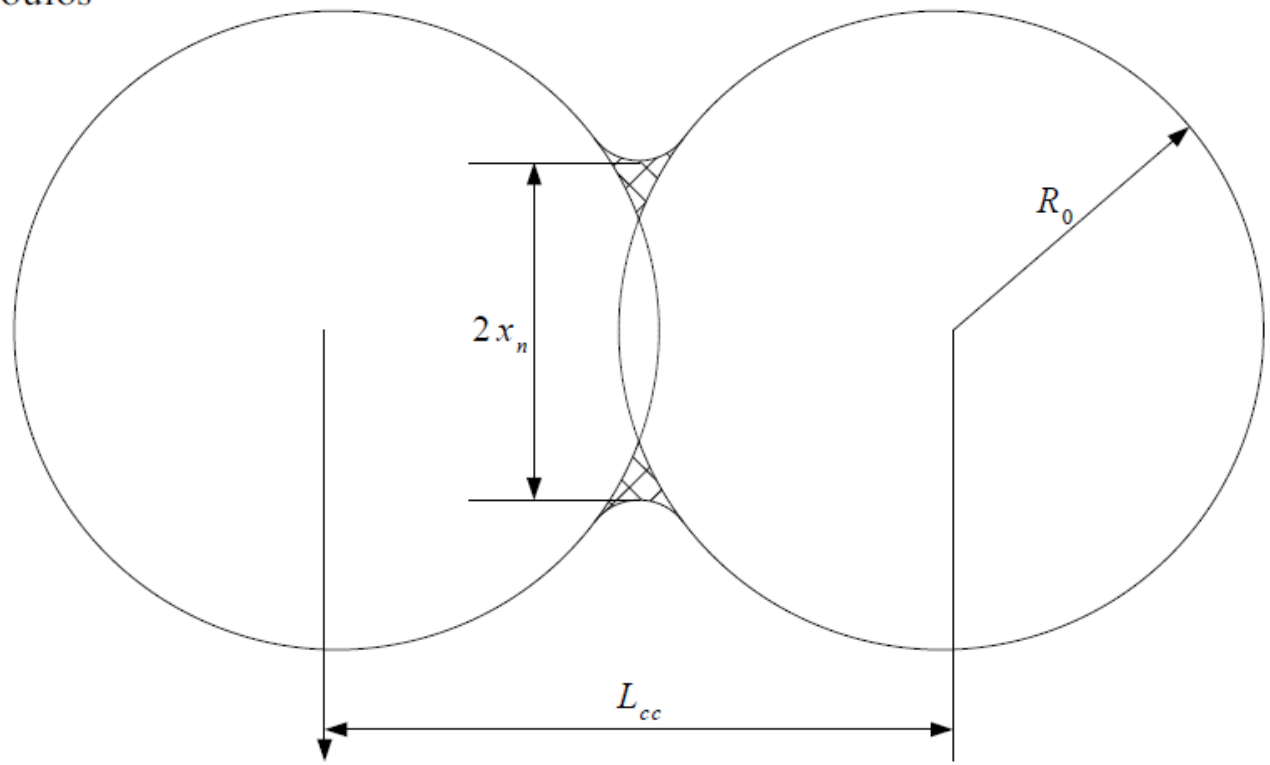

Figure 7.2: The geometry of two sintering nanoparticles. The shaded area is the neck region

The initial growth stage of sintering is best described by the neck growth in terms of the neck radius. Frenkel [128] and Kuczinski [129] pioneered studies in this direction. For two tangent spherical particles with the equal size, the neck growth equation resulted by any individual mass transport mechanism is given as

Free-standing nanoparticles
Evoluzione temporale di x_n
Non restituisce evoluzione temporale di R

$$\left(\frac{x_n}{R_0}\right)^n = \frac{B(T)}{R_0^m} t \qquad (6.24)$$

where $B(T)$ is a term depending on the sintering temperature and relevant material properties and t is the time. The exponent m and n depend on the specific dominant mass transport mechanism. The characteristic coalescence time τ_f is defined from Eq. (6.24) as the time at which the neck radius to the particle initial radius ratio reaches 1 or 0.83 (corresponding to the largest possible neck to radius ratio of two sintering spheres). For

the surface diffusion, Nichols and Mullins [130][131] showed that

$$B(T) = \frac{25 D_s \gamma_s \delta^4}{k_B T};\ m = 4;\ n = 6;\ \tau_f = R_0^4 / B(T) \tag{6.25}$$

where D_s is the surface diffusion coefficient and δ is the atomic size. For the grain boundary diffusion, Coblentz *et al.* [132] gave the expression

$$B(T) = \frac{192 D_g b \gamma_s \delta^3}{k_B T};\ m = 4;\ n = 6;\ \tau_f = R_0^4 / B(T) \tag{6.26}$$

where D_g is the grain boundary diffusion coefficient and b is the width of the grain boundary.

The diffusion coefficient is assumed to follow the Boltzmann–Arrhenius dependency:

$$D = D_0 \exp(-E_a/RT)$$

where D_0 is the pre-exponential diffusion coefficient and E_a the activation energy.

Assuming grain boundary diffusion as the driving phenomenon (Nakaso et al., 2002), the proper pre-exponential factor and the activation energy can be calculated with the empirical relationship deduced from experimental data of bulk material valid for fcc crystal structures (Gjostein, 1972):

$$D_0 = 0.3 \text{ cm}^2/\text{s} \tag{8}$$

$$E_a = 47.5 \cdot T_M \text{ J/mol} \tag{9}$$

where T_M is the bulk melting temperature.

The surface tension is calculated using the relation of Murr (1975) for pure fcc metals:

$$\sigma_{sv} \simeq 1.2(\sigma_{lv})_M + 0.45(T_M - T) \tag{10}$$

where $(\sigma_{lv})_M$ is the surface tension of liquid bulk gold at the melting point.

Table 4.1. Coalescence time for two silver particles with $R = 10$ nm

Temperature T [K]	Volume diffusion t_{co}	Grain boundary diffusion t_{co}
298		5 years
373	15 years	25 days
473	21 min	1 days
573	0.3 s	4 min
673	0.9 ms	20 s

Activation energy volume diffusion<Activation energy grain boundary diffusion

PHYSICAL REVIEW A VOLUME 44, NUMBER 12 15 DECEMBER 1991

Growth of droplets on a substrate by diffusion and coalescence

A. Steyer, P. Guenoun, and D. Beysens
Service de Physique du Solide et de Résonance Magnétique, F-91191 Gif-sur-Yvette CEDEX, France

C. M. Knobler
Department of Chemistry and Biochemistry, University of California at Los Angeles, Los Angeles, California 90024
(Received 5 March 1991)

This paper is devoted to the theoretical and numerical investigation of growth phenomena on a substrate in the case where diffusion and coalescence play the major roles. Such phenomena, where clusters of given dimensionality (D) nucleate and develop on a substrate of lower dimensionality (d) are found in many areas of fundamental and applied sciences (heterogeneous nucleation, thin-film growth, heat and mass transfer) and daily occurrences, like the formation of dew. Understanding the underlying

At this stage, the growth of the droplets leads to a continuous increase in surface coverage. When the interactions by coalescence become important, growth is accelerated, and the average droplet radius behaves as

$$\langle R \rangle \sim t^{1/(D-d)} . \tag{2}$$

Study of the coalescence process of SiO_2 supported Au NPs

Data analysis: size-dependent activation energy

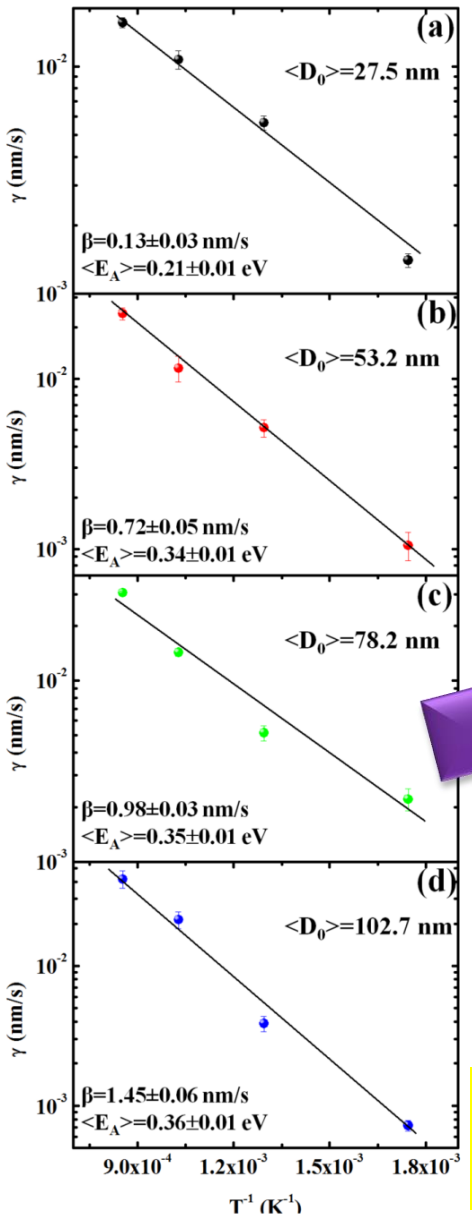

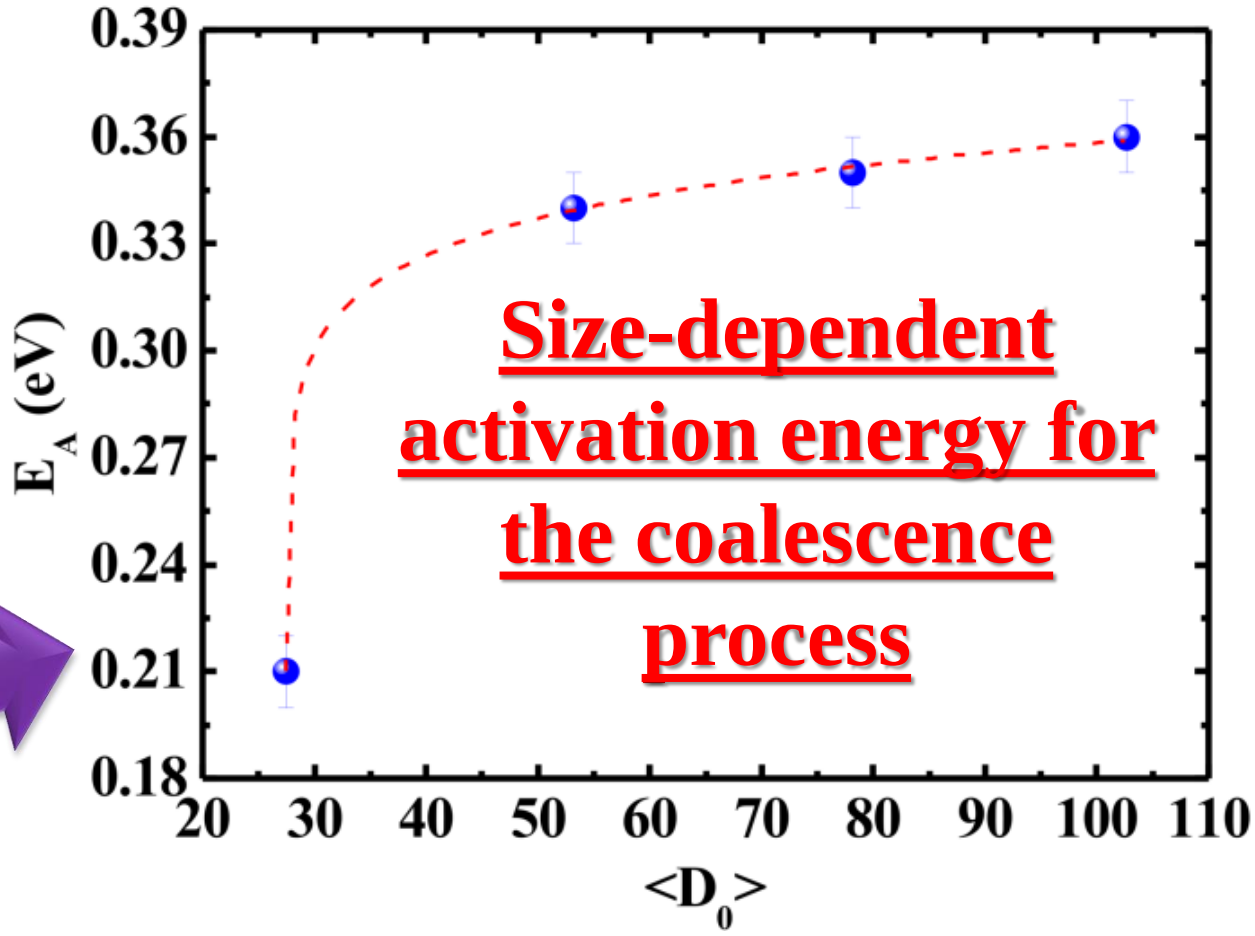

$$\gamma = \beta \exp[-E_A / kT]$$

F. Ruffino et al. Physica E 74, 388 (2015)

Study of the coalescence process of SiO_2 supported Au NPs

Data analysis: considerations

The values estimated by us in the 0.21-0.36 eV are compatible, mainly, with Au self-diffusion involved in the NPs coalescence process

- $E_A \approx 0.4$ eV is characteristic of Au atoms surface self-diffusion (H. Göbel, P. von Blanckenhagen, Surf. Sci. 331-333 (part B) (1995) 885).

- $E_A \approx 1$ eV is characteris f-diffusion (T. S. Lin, Y. W. Chung, S uctures 4 (1988) 709).

- $E_A \approx 0.7$ eV is characte undary (S. Arcidiacono et al., Int 004) 979).

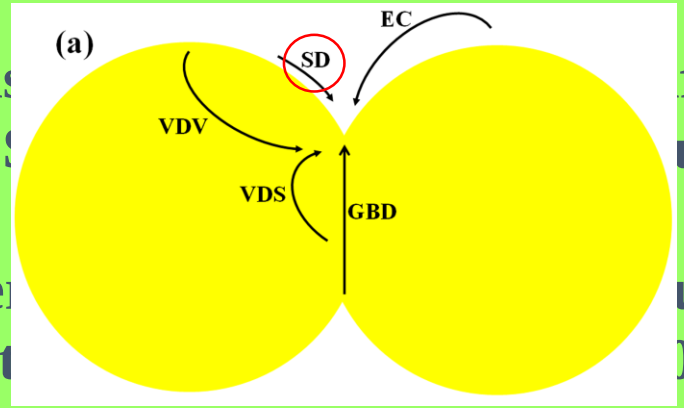

Study of the coalescence process of SiO_2 supported Au NPs

Considerations on the size-dependent activation energy

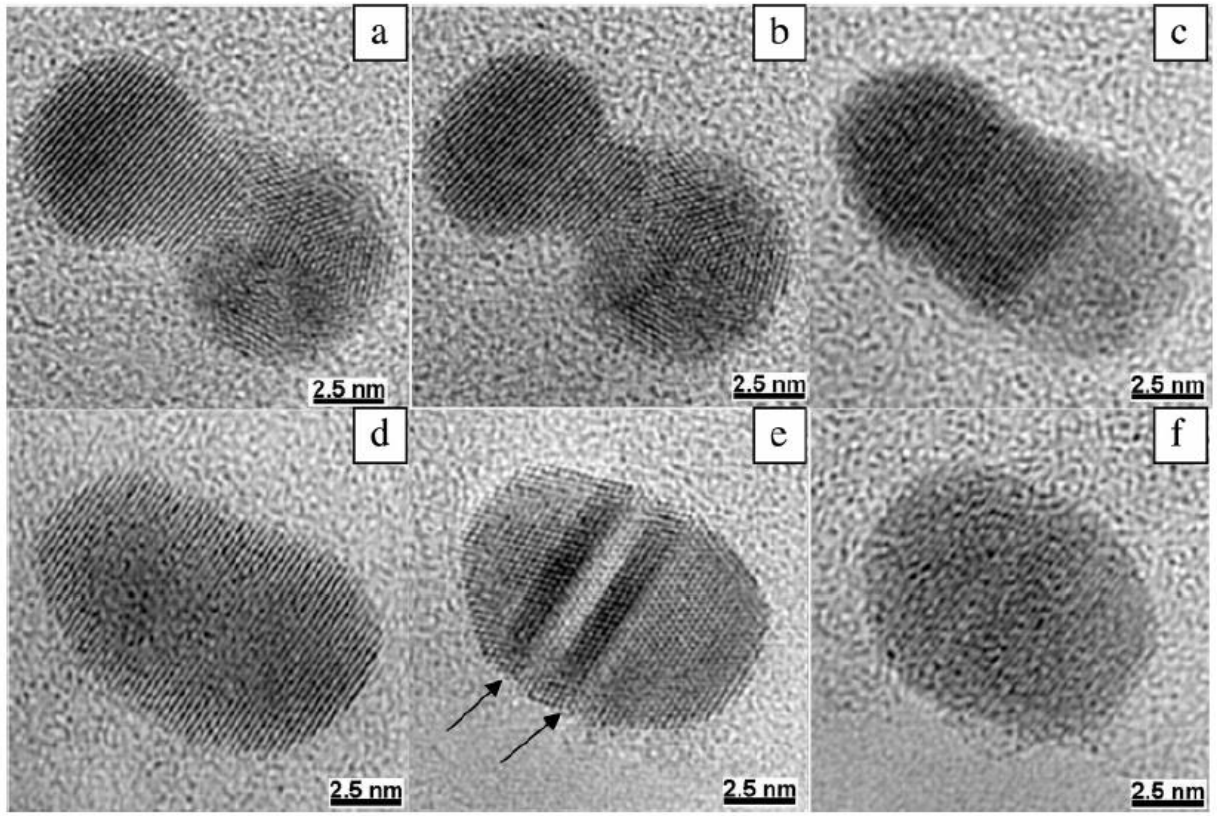

M. José-Yacamán et al., J. Phys. Chem. B 109, 9703 (2005):

In-situ (TEM) observation of the thermal induced coalescence of two Au NPs. (a, b) Neck formation at the contacting surfaces. (c, d) Crystal planes alignment. (d) Plane defects formation in the new stressed structure. (f) The newly formed structure is now relaxed.

"The coalescence process begins with NPs contact, followed by the alignment of the coalescing planes at the interface between the nanoparticles; the liquidlike mobility of the nanoparticle surface layers is essential to achieve this. When a small particle coalesces with a larger one, the smaller one rotates to orient its planes to those of the larger one".

NPs surface melting as essential condition to coalescence

Our data confirm the finding of José-Yacamán et al.: essential role of a high-mobility (liquid-like behavior) of the NP surface atoms for the coalescence process.

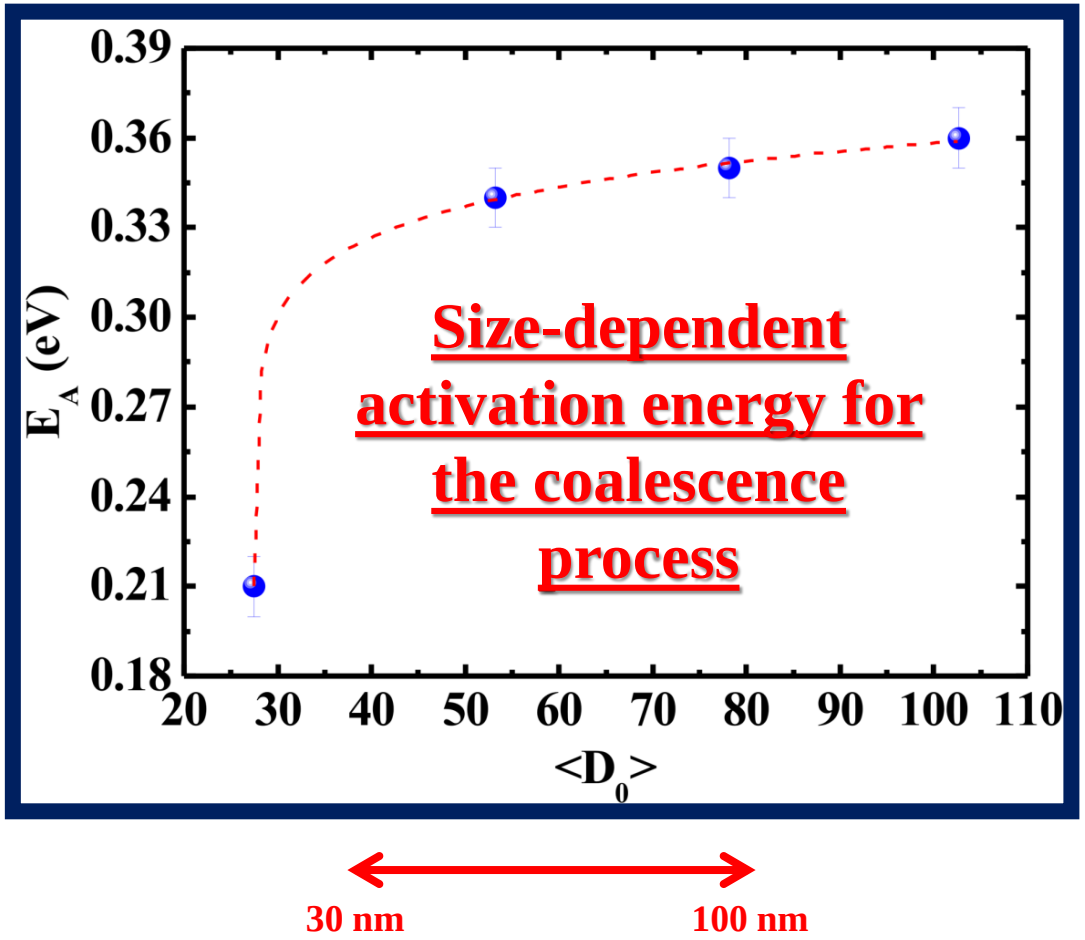

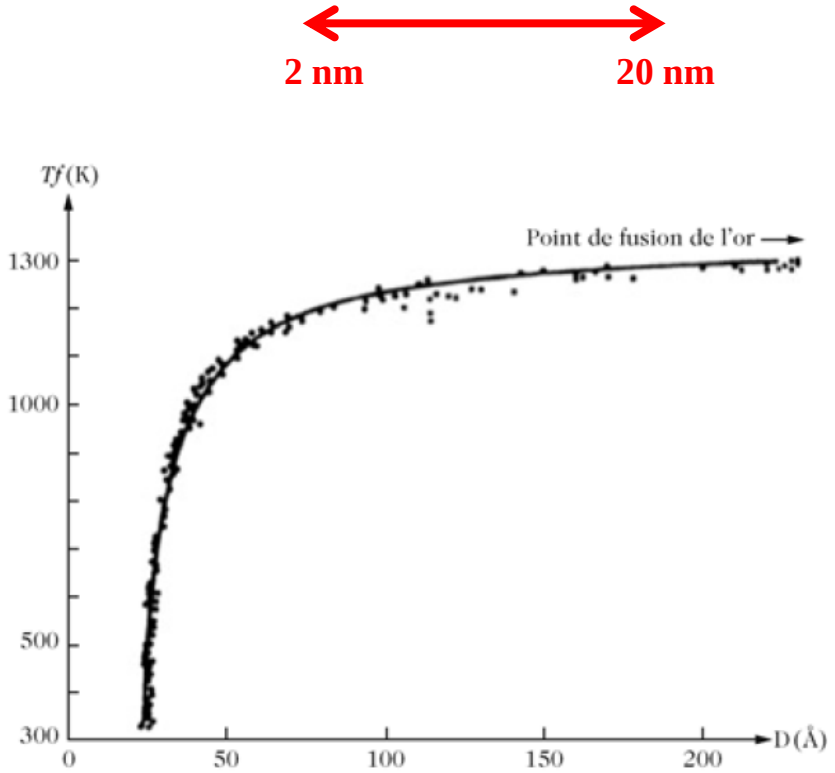

Fig. 3.3. Dependence of the solid–liquid transition temperature of gold on particle diameter. Taken from [4]. The transition is detected by the disappearance of Bragg peaks in the electron diffraction pattern. *Dots* represent experimental values. The *continuous curve* is fitted to (3.3) by the least squares method

A case in which both nanoparticles ripening and coalescence act

Electron beam irradiation (in-situ by TEM),
200 keV, **$1.8\times10^3 \div 1.62\times10^4$ C/cm^2**

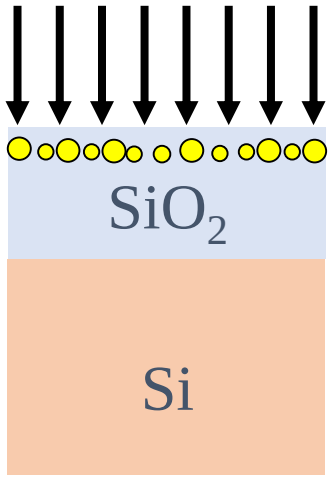

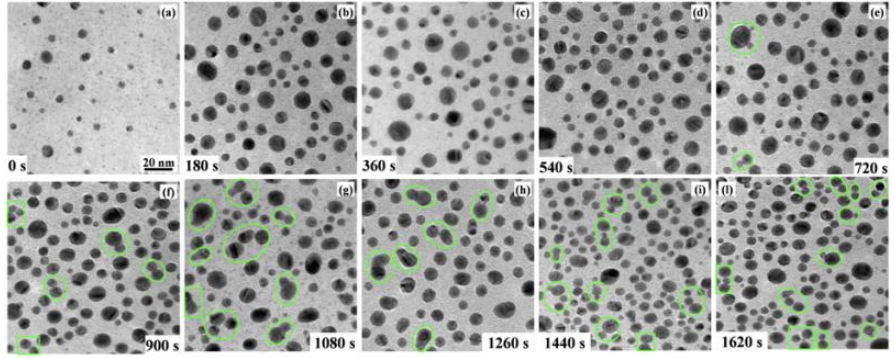

F. Ruffino et al., *J. Phys. D 42, 075304 (2009)*

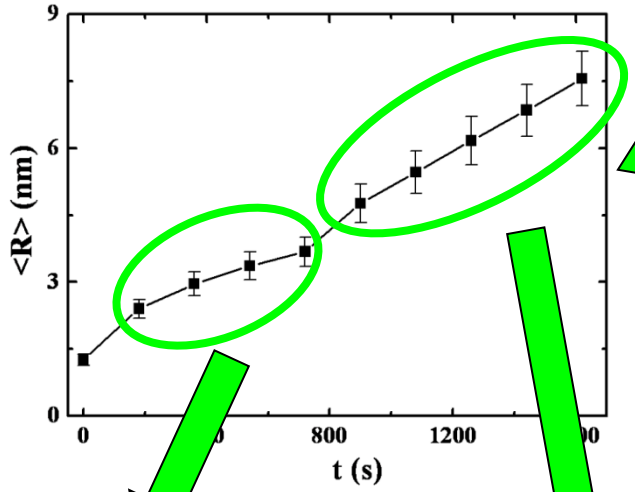

$$R^3(t) - R_0^3 = Kt$$

$$D_I(25°C) = 2.4\times10^{-8} cm^2/s$$

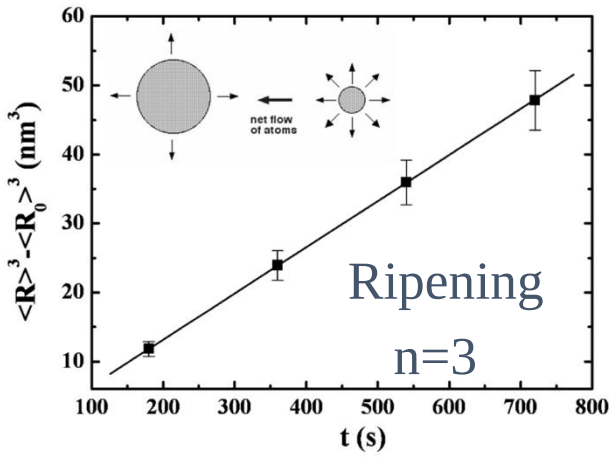

Ripening
n=3

$$R(t) - R_0 = K^* t$$

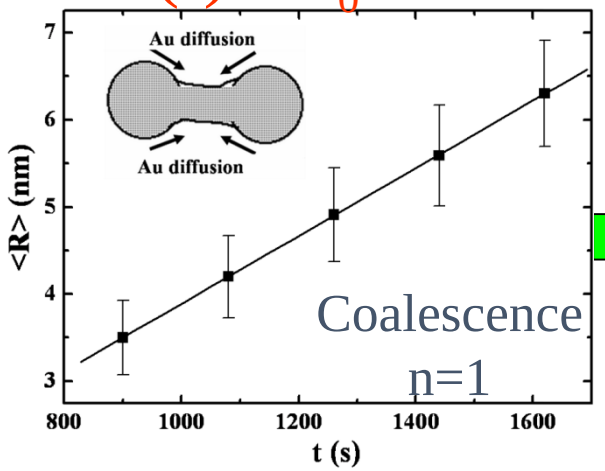

Coalescence
n=1

Coalescence mechanism

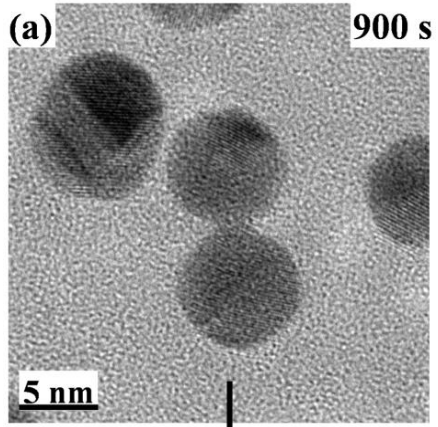

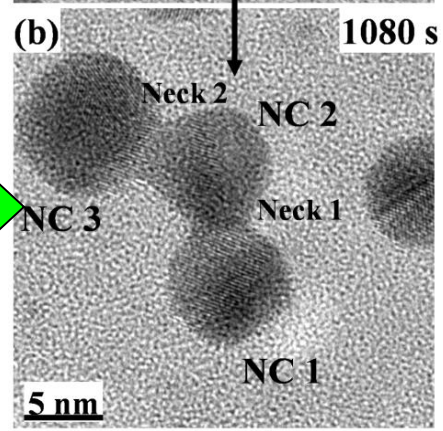

More in depth: rate equations for ripening and for coalescence

Rate equation

JOURNAL OF MATERIALS SCIENCE 37 (2002) 2171–2202

Review
Progress in Ostwald ripening theories and their applications to nickel-base superalloys

Part I: *Ostwald ripening theories*

A. BALDAN
Department of Metallurgical and Materials Engineering, Mersin University, Ciftlikkoy, Mersin, Turkey
E-mail: abaldan@mersin.edu.tr

A major advance in the theory of Ostwald ripening was made in a paper by Lifshitz and Slyozof [5, 6] and followed by a related paper by Wagner [7] (LSW). In contrast to previous theories, The LSW developed a method for treating an ensemble of dilute coarsening particles, and were able to make quantitative predictions on the long-time behavior of coarsening systems without recourse to a numerical solution of the relevant equations. The limitation of infinite dilution al-

Thermodynamic driving force for ripening

Competitive growth takes place among precipitates when particles with various sizes are dispersed in a matrix. The growth originates from the concentration gradients around the particles caused by the thermodynamic demand, i.e. the Gibbs-Thomson equation: the concentration at the surface of particles in equilibrium with larger particles is lower than that with smaller particles. Solute atoms flow through the concentration gradients both from the surface of the smaller particles to matrix and from the matrix to the surface of larger particles. During this process, average radius of the particles increases. The phenomena can take place in any stage of precipitation.

Any system of disperse particles statistically distributed in a medium and possessing certain solubility in it will be thermodynamically unstable due to a large interface area. Its decrease in approaching equilibrium is accompanied by particle coarsening whose solubility depends on their radii and is described by the well known Gibbs-Thomson relation

$$C_r = C_e \exp\left[\frac{2\gamma\Omega}{R_B T} \cdot \frac{1}{r}\right] \approx C_e\left[1 + \frac{2\gamma\Omega}{R_B T} \cdot \frac{1}{r}\right] \quad (1)$$

where C_e is the solute concentration at a plane interface in the matrix in equilibrium with particle of infinite radius, C_r is the solubility at the surface of a spherical particle with radius r, γ is the specific interfacial energy of the matrix-precipitate particle boundary, Ω is the mean atomic (or molar) volume of the particle, R_B is the Universal gas constant [8.314×10^3 J /(K. kmol)] and T is the absolute temperature. The difference between C_r and C_e induces a diffusive flux of atoms from the smaller to the larger particles. Thus the average particle radius increases and the total number of particles decreases with time, as well as the total free surface enthalpy of the system.

The kinetic equation is usually the difficult to determine for it is based upon a solution to a potentially difficult free-boundary problem. The concentration field equation describing mass flow, which must be solved in both phases, is

$$\nabla^2 C = 0 \tag{5}$$

If particles flow through particle size space in a continuous manner, the time rate of change of the number of particles per unit volume of size R to $R + \mathrm{d}R$, $f(R, t)$, is given [19] by the flowing continuity equation

$$\frac{\partial f}{\partial t} + \frac{\partial (f\ \mathrm{d}R/\mathrm{d}t)}{\partial R} = 0 \tag{9}$$

where $\mathrm{d}R/\mathrm{d}t$ is the growth or shirinkage rate of a particle as given by the kinetic equation, and t is time. The

The mass conservation equation implies that if the mean-field condition is a function of time during ripening, then the mole fraction of the second phase particle Q must also be a function of time. The mole fraction, is related to the particle size distribution function $f(R, t)$ as

$$Q = G \int_0^\infty R^3 f(R, t)\, \mathrm{d}R \tag{11}$$

where G is a geometrical factor that depends on the particle morphology.

The major advance in the theory of ripening was made in a paper by Lifshitz and Slyozov [3.15] and followed by a related paper by Wagner [3.16]. In contrast to previous theories, LSW developed a method for treating an ensemble of dilute coarsening particles, and were able to make quantitative predictions on the long-time behavior of coarsening systems without recourse to a numerical solution of the relevant equations. The LSW theory is valid when the volume fraction of dispersed phase is sufficiently small. When volume fraction of dispersed phase becomes larger, the factor of the growth rate becomes large and this volume effect will accelerate Ostwald ripening. Because we will use the LSW theory to model the growth rate of the particles, it is assumed that volume fraction of the dispersed phase is sufficiently small. The diffusion equation in terms of the concentration $C(\vec{r},t)$ of the dispersed phase component in the diffusive medium at a give time t and in space at coordinate $\vec{r}$ can be written:

$$\frac{\partial C(\vec{r},t)}{\partial t} = D\nabla^2 C(\vec{r},t) + F \tag{3.10}$$

where D denotes the diffusion coefficient and F the amount of component consumed by grain growth or evolved by dissolution per unit volume and time:

$$F = -\left(\frac{4\pi}{\bar{\nu}}\right)\int f(R)\frac{dR}{dt}R^2 dR \tag{3.11}$$

with $f(R)$ the size distribution function [3.13], R the radius of a particle, $\bar{\nu}$ the molar volume of the dispersed phase. Now, it is necessary to consider the Gibbs-Thompson effect described by the Gibbs-Thompson equation (capillary approximation):

$$C_R = C_e e^{\frac{2\gamma\Omega}{k_B T}\frac{1}{R}} \approx C_e\left[1+\frac{2\gamma\Omega}{k_B T}\frac{1}{R}\right] = C_e\left[1+\frac{R_C}{R}\right] \tag{3.12}$$

where C_e is the solute concentration at a plane interface in the matrix in equilibrium with particle of infinite radius, C_R is the solubility at the surface of a spherical particle with radius R, γ is the specific interfacial energy of the matrix-precipitate particle boundary, Ω is the mean atomic volume of the particle, T the absolute temperature and $R_C = 2\gamma\Omega / k_B T$ is usually referred as the capillary length. The difference between C_R and C_e induces a diffusive flux of atoms from the smaller to the larger particles. Thus, the average particle radius increases and the total number of particles decreases with time, as well as the total free surface enthalpy of the system. This equation express the thermodynamic driving force for ripening.
Lifshitz and Slyozov represented the growth rate of a particle due to ripening as

$$\frac{dR}{dt} = \bar{\nu} D \frac{\left(C(\vec{r},t) - C_R\right)}{R} \tag{3.13}.$$

This growth rate results from the stationary solution of the diffusion field around a single spherical particle with radius R. Such an equation is based on the critical assumption that the particle coarsening rate is independent of its surrounding. This is tantamount to a "mean field" description

of the particle's growth rate. The eqs. (3.10)-(3.13) are the basis for Ostwald ripening process of particles dispersed in a matrix. In particular, basing on such equations it is possible to determine the temporary evolution of the average radius $R(t)$ of the particles in stationary state (i. e. for sufficiently high time) as [3.9]:

$$R^n(t) - R_0^n = K^* t \tag{3.14}$$

with R_0 the radius of the particle at time $t = 0$, and K^* an appropriate constant depending on the diffusion coefficient [3.17]. In particular, the fundamental formulations of the ripening theory differ themselves by the value of the exponent n [3.9]:

- $n = 2$ (2D/2D case) for the growth of two-dimensional (2D) particles on a surface (2D);
- $n = 3$ (3D/3D case) for the growth of the three-dimensional (3D) particles embedded in a bulk matrix (3D);
- $n = 4$ (3D/2D case) for the growth of three-dimensional (3D) particles on a surface (2D).

The ripening mechanism is a process mediated by the diffusion of clusters component from the clusters with $R < R^*$ to the clusters with $R \geq R^*$. About the atomic diffusion process (in the bulk or on a surface), we recall simply that it is described by a diffusion coefficient D. The Fick's first law relate the atomic flux J to the atomic gradient concentration (the driving force of the process). In one dimension: $J = -D(\partial C / \partial x)$.
The Fick's second law (continuity equation) describe the temporal variation of atomic concentration. In one dimension: $(\partial C / \partial t) = D(\partial^2 C / \partial x^2)$. The diffusion coefficient, in general, is found to have an activated Arrhenius form [3.5]:

$$D = D_0 \exp\left(-\frac{E_a}{k_B T}\right) \tag{3.15}$$

with E_a the characteristic activation energy of the diffusion process.

2) The coalescence process: quantitative details

IOP PUBLISHING NANOTECHNOLOGY

Nanotechnology **21** (2010) 025701 (6pp) doi:10.1088/0957-4484/21/2/025701

Coalescence and sintering of Pt nanoparticles: *in situ* observation by aberration-corrected HAADF STEM

M A Asoro[1], D Kovar[1,2], Y Shao-Horn[3,4], L F Allard[5] and P J Ferreira[1,2]

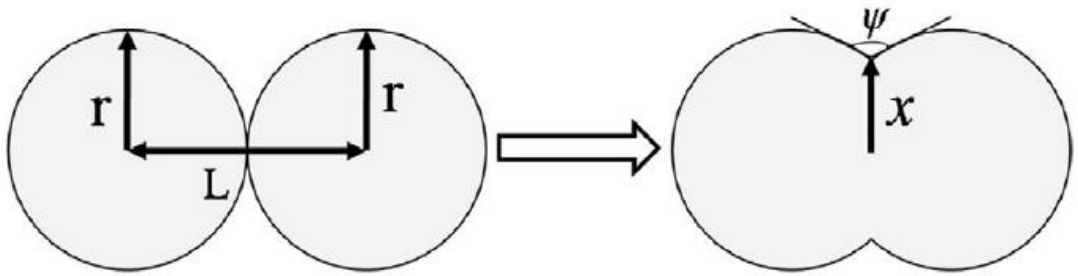

Figure 1. Schematic of sintering of a pair of spherical particles. r is the particle radius, L is the center-to-center distance, x is the neck radius and ψ is the dihedral angle.

To understand the sintering process, we consider that, during the early stages of sintering, neck growth occurs to reduce the chemical potential at the particle contact points (figure 1). Possible mass transport mechanisms for neck growth include grain boundary diffusion, surface diffusion and lattice diffusion, as well as deformation. We focus on the diffusion mechanisms as they likely dominate the sintering behavior of nanoparticles. Indeed, it is unlikely that dislocation-driven plastic flow would contribute significantly to neck growth in face centered cubic (fcc) nanoparticles, given the large stresses required for plastic flow in a nanoparticulate system [10].

The ratio of neck size, x to particle radius, r during the initial stages of sintering between two uniformly sized particles is given by [5, 6, 11]

$$\frac{x}{r} = \left(\frac{Ft}{r^n}\right)^{1/m} \tag{1}$$

and the densification (characterized by the shrinkage between the particles' centers) is given by

$$\frac{\Delta L}{L} = \left(\frac{-Ft}{2^m r^n}\right)^{2/m} \tag{2}$$

where t is the sintering time, L is the center-to-center distance between particles and F, m, and n depend on the dominant sintering mechanism (see table 1). Note that $\Delta L/L = 0$ when surface diffusion is dominant since this is a non-densifying diffusion mechanism.

Table 1. Values for the variables in equations (1) and (2). D_s, D_l and D_{gb} are the diffusion coefficients for surface, lattice and grain boundary diffusion, respectively. δ_s and δ_{gb} are the thicknesses for surface and grain boundary, respectively. γ_s is the surface energy. Ω is the atomic volume. From [11].

Mechanism	m	n	F
Surface diffusion	7	4	$\frac{56 D_s \delta_s \gamma_s \Omega}{KT}$
Grain boundary diffusion	6	4	$\frac{96 D_{gb} \delta_{gb} \gamma_s \Omega}{KT}$
Lattice diffusion from the surface	4	3	$\frac{20 D_l \gamma_s \Omega}{KT}$
Lattice diffusion from the grain boundary	5	3	$\frac{80\pi D_l \gamma_s \Omega}{KT}$

Sintering /coalescence process is accepted as a thermal treatment for bonding particles into a coherent, predominantly solid structure via mass transport events that often occur on the atomic scale [125]. It is traditionally used for manufacturing ceramic is still poorly understood. According to the continuum theory, the driving force is believed to be the excess surface free energy in the system. While various mass transport models have been proposed to describe the sintering process for microparticles [125], high sintering rates observed at low temperatures for nanoparticles cannot be explained by any diffusion-based model. Due to the high surface-to-volume ratio, the nanoparticle temperature can be significantly altered by surface energy release, which turns out to accelerate the sintering/coalescence process. Besides this, the melting temperature of nanoparticles is well known to be size-dependent, leading to a complex melting/solidification process when coalescence of nanoparticles is initiated at the temperature slightly below a nanoparticle melting temperature.

7.2.1 Mass transport mechanism

The driving force for sintering/coalescence process is believed to be the excess surface free energy in the system. Local curvature changes during the coalescence process create the corresponding gradients in vapor pressure, chemical potential or surface stress over neighboring surfaces, and promote the motion of atoms and vacancies [125]. Various mass transport models are proposed to describe ways of material migration in the sintering particles. In the solid-state, these include surface diffusion (SF), grain boundary diffusion (GBD), evaporation & condensation (EC), and volume diffusion from the surface of the particle (VDS) and from the interior of the particle (VDV). In the liquid or amorphous material, viscous flow (VF) is often considered as the dominant mechanism. These models have been extensively reviewed in the dissertation of Lunden [127], and are illustrated in Figure 7.1 together with their transport paths.

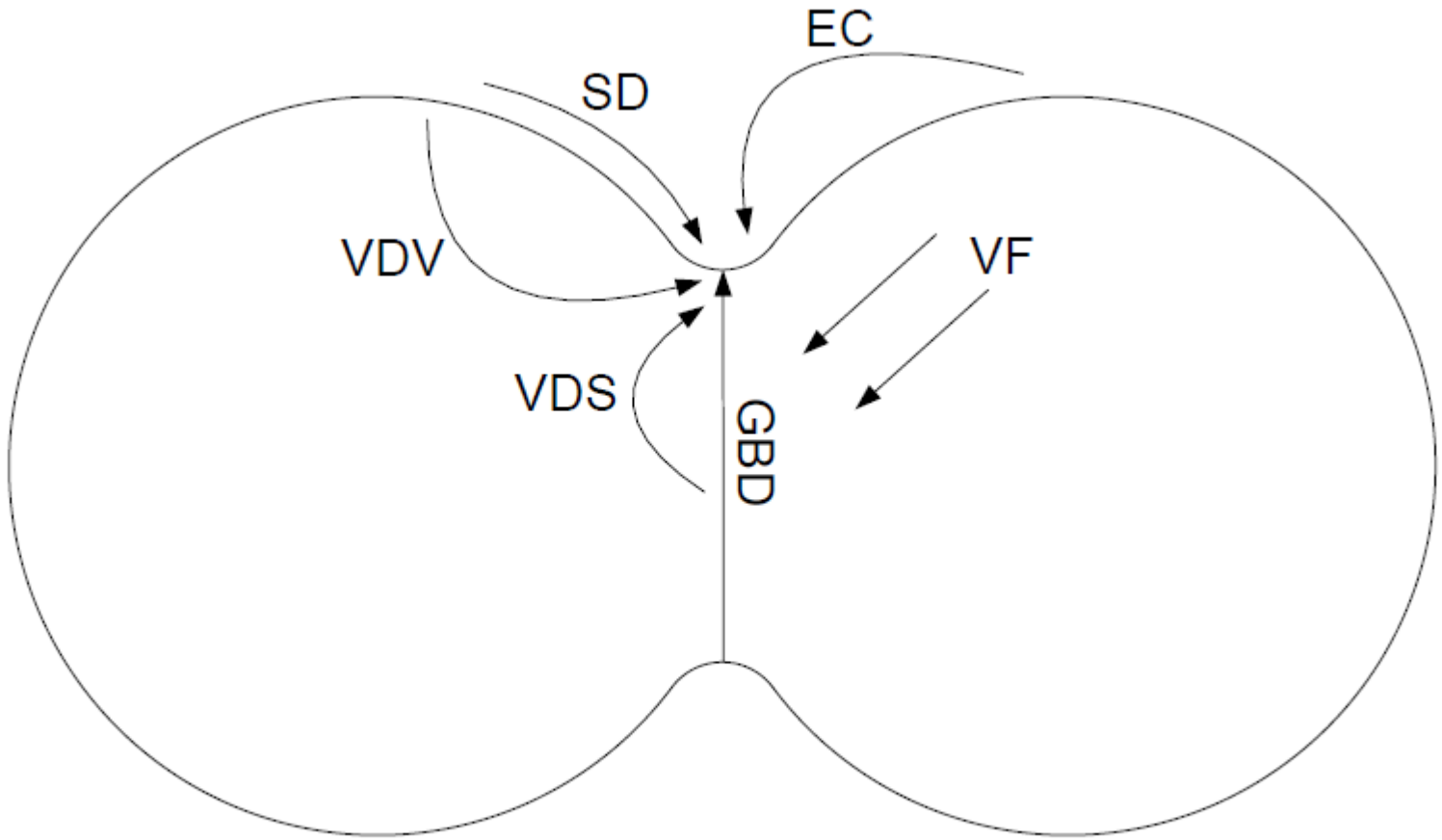

Figure 7.1: Six mass transfer mechanisms and their transport paths

Generally speaking, the material migration mechanisms during the sintering process can be grouped into two categories. In the EC, SD and VDS models, material is transported from the particle surface toward the neck, simply filling the area between particles. However, the particle mass centers remain at the same location. These mechanisms are called adhesion mechanisms. On the other hand, in the GBD, VDV and VF models, materials are moved from the region between the particles toward the neck, causing the particle mass centers approach one another. These mechanisms are called densification mechanisms.

7.2.2 Morphology evolution of sintering particles

The morphology evolution of two sintering particles can be divided into two stages. In the initial growth stage, two spherical particles approach each other driven by various gradients between them and the neck region is created. This process is shown in Figure 7.2, where x_n is the neck radius and R_0 is the initial particle radius. A larger spheroidal particle is formed in the end. In the second coalescence stage, the non-spherical particle gradually changes into a spherical particle.

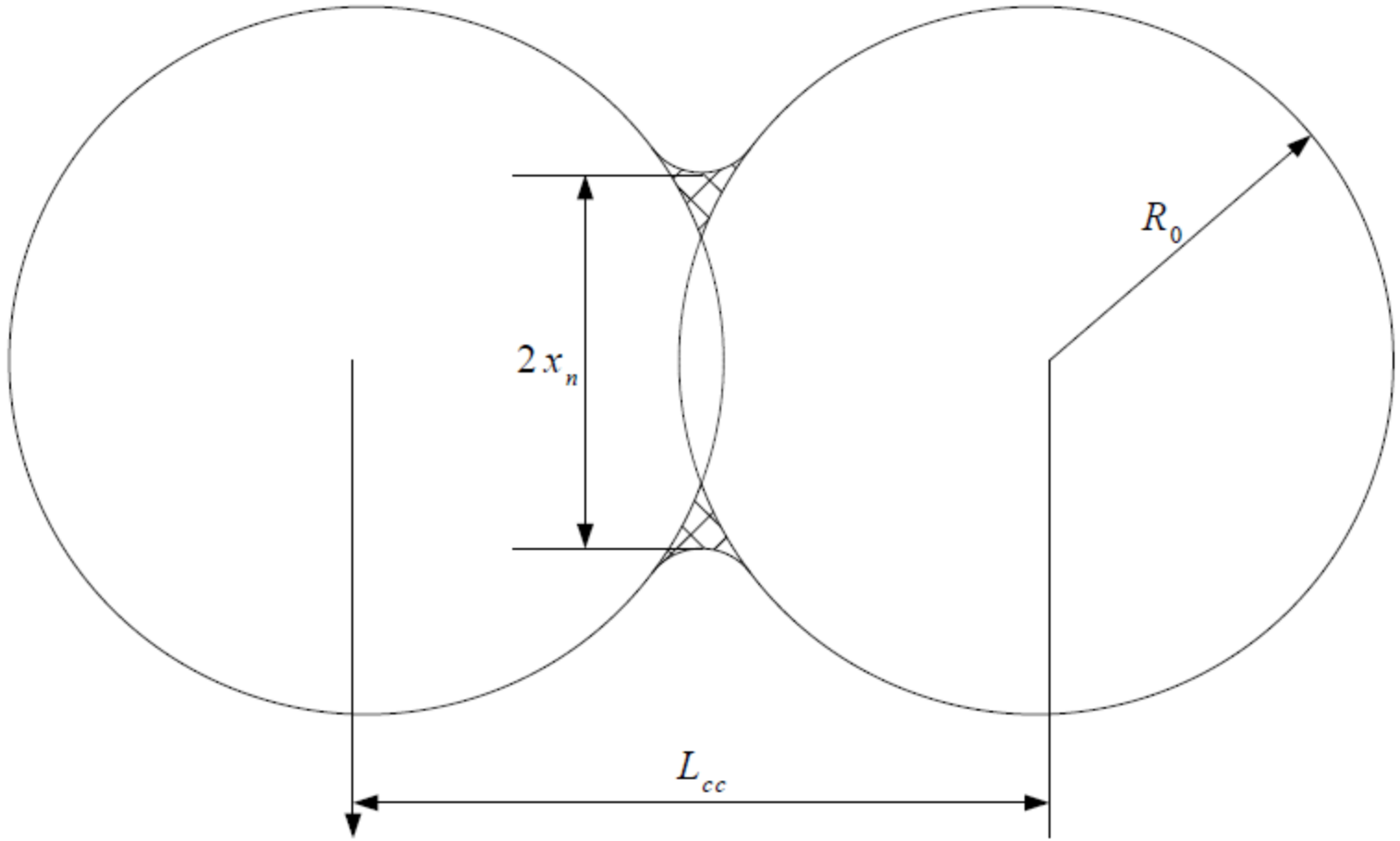

Figure 7.2: The geometry of two sintering nanoparticles. The shaded area is the neck region

The initial growth stage of sintering is best described by the neck growth in terms of the neck radius. Frenkel [128] and Kuczinski [129] pioneered studies in this direction. For two tangent spherical particles with the equal size, the neck growth equation resulted by any individual mass transport mechanism is given as

$$\left(\frac{x_n}{R_0}\right)^n = \frac{B(T)}{R_0^m} t \tag{6.24}$$

where $B(T)$ is a term depending on the sintering temperature and relevant material properties and t is the time. The exponent m and n depend on the specific dominant mass transport mechanism. The characteristic coalescence time τ_f is defined from Eq. (6.24) as the time at which the neck radius to the particle initial radius ratio reaches 1 or 0.83 (corresponding to the largest possible neck to radius ratio of two sintering spheres). For

the surface diffusion, Nichols and Mullins [130][131] showed that

$$B(T) = \frac{25 D_s \gamma_s \delta^4}{k_B T};\ m = 4;\ n = 6;\ \tau_f = R_0^4 / B(T) \tag{6.25}$$

where D_s is the surface diffusion coefficient and δ is the atomic size. For the grain boundary diffusion, Coblentz *et al.* [132] gave the expression

$$B(T) = \frac{192 D_g b \gamma_s \delta^3}{k_B T};\ m = 4;\ n = 6;\ \tau_f = R_0^4 / B(T) \tag{6.26}$$

where D_g is the grain boundary diffusion coefficient and b is the width of the grain boundary. While for the viscous flow, Frenkel [128] developed a simple model as

$$B(T) = \frac{3\gamma_l}{2\pi\eta};\ m = 1;\ n = 2;\ \tau_f = R_0 / B(T) \tag{6.27}$$

where η is the viscosity.